A Study of a Coordinated Path Planning Strategy for a Fleet of Unmanned Surface Ships in the Presence of Static Obstacles

By

MARO JEON

Submitted for the degree of Master of Philosophy

Department of Naval Architecture, Ocean and Marine Engineering

University of Strathclyde

January 2018

Declaration of Authenticity and Author's Rights

This thesis is the result of the author's original research. It has been composed by the author and has not been previously submitted for examination which has led to the award of a degree.

Signed:

Date: January 2018

Acknowledgements

I would like to express my gratitude and sincere thanks to my supervisor Mr. David Clelland of the Department of Naval Architecture, Ocean and Marine Engineering at University of Strathclyde. He always kept providing me with the opportunity to research this study and for supervising my work throughout a whole year.

Sincere appreciation also goes to my Korean supervisor Prof. Sang-Hyun Kim at Inha University. He provided the first step to study at Strathclyde University and keep supporting and encouraging me. It was a great help to me enduring a difficult time during my study.

Finally, I would like to thank my colleagues at the laboratoryfor their advice and encouragement during my work. This project would have been impossible without them.

Sincerely thanks to all.

Maro Jeon

Abstract

This thesis addressed the problem of path planning for a fleet of unmanned surface ships in the presence of static obstacles. The aim of this study is to propose a new strategy to avoid potential collisions with static obstacles and each ship. In addition, the objective of the proposed strategy is to enable the fleet to autonomously change an initial formation shape into a safer formation shape when the fleet of the ships faces with static obstacles. A core idea adopted for the proposed strategy was motivated by behaviours of school of fish in the ocean. We assumed that the behaviours of school of fish follow three rules. These assumptions were extended to main methodology of this study: 1) Path planning for a leader ship (***Potential Field Method***), 2) Formation control for a fleet (***Consensus algorithm***) and 3) Path planning strategy for follower ships of a fleet. In addition, ***Potential Field Method*** and ***Consensus algorithm*** were integrated to develop the new path planning strategy, which imitates the motion of school of fish when obstacles are encountered. Repulsive force vectors obtained from results of ***Potential Field Method*** were used as parameters of proposed mathematical equations to change formation shapes of the fleet. In order to validate the proposed strategy, simulations have been carried out for five unmanned surface ships modelled as point mass models with full actuation under MATLAB/Simulink environment. Simulation results illustrated that the fleet of the five ships changed their formation shape into a safer formation shape in the presence of user-designed static obstacles and the fleet of ships successfully passed through the static obstacles without collisions with each ship. From these simulation results, this study has demonstrated that this proposed strategy will contribute to safety and automation of multiple unmanned surface ships in the presence of static obstacles.

Key words: Unmanned surface ships, Path planning, Formation control, Potential field method (PFM), Consensus algorithm

Contents

Acknowledgements 3

Abstract 4

Chapter 1. Introduction 7

1.1. Background 7

1.2. Motivation 7

1.3. Aim and objectives 8

1.4. Approach 9

1.5. Layout of Thesis 10

Chapter 2. Literature review 11

2.1. Overview of formation control 11

2.2. Formation control approaches in the presence of obstacles 13

2.3. Coordinated formation strategies in the presence of static obstacles 15

Chapter 3. Methodology 18

3.1. Path planning for a leader 18

3.1.1. Potential field method (PFM) 19

Attractive potential function 19

Repulsive potential function 20

3.1.2. Gradient descent 22

3.1.3. Example 23

3.2. Formation control 28

3.2.1. Consensus algorithm 28

3.2.2. Example 29

3.3. Coordinated path planning strategy 32

3.3.1. Repulsive force vector by potential field method 33

3.3.2. Types of formation shapes 34

3.3.3. Coordinated path planning strategy by repulsive force vector 35

3.4. Examples 38

Chapter 4. Simulation 43

4.1. Basic configuration of simulations 43

4.1.1. Map representation 43

4.1.2. Initial setup for simulations 44

4.2. Simulation results 45
4.2.1. Case1: Simulation result 45
4.2.2. Case2: Simulation result 50
Chapter 5. Discussion, Conclusion and Further Work 51
REFERENCES 53
Appendix A 55
Appendix B 57
Appendix C 61
Appendix D 64
Appendix E 66

Chapter 1. Introduction

1.1. Background

Today, there has been increased in the importance of unmanned surface ships since most of the accidents and fatalities at sea happen on-board because of human error. In addition, unmanned surface ships have many of advantages in safety and efficiency.

Historically, unmanned surface ships were firstly developed in 1946 for naval purposes. Since 1946, there have been a lot of studies on unmanned surface ships for military, commercial purposes as well as for tasks such as surveillance, surveying, and exploration.

Nowadays, fully autonomous unmanned surface military vessels in Norwegian company Yara are expected to be developed in 2020. Autonomous unmanned ocean-going commercial ships in Rolls-Royce are aimed to be operated in 2035. However, most studies have focused on a single surface ship that has a lack of payload capacity and deficiency in mission achievement.

In order to improve the weakness of a single ship, the recent and future trend of unmanned surface ships is to bring into effective action a fleet of unmanned surface ships in a formation to achieve cooperative tasks. The advantages of formation control of multiple unmanned surface ships include wide-range mission area, enhanced system robustness, and higher efficiency (Fan, Feng et al. 2010), (Liu, Bucknall 2015).

However, there are a few problems to be considered on formation control of a fleet of unmanned surface ships. When a fleet of ships move towards a goal in the presence of obstacles, the main considerations are how to avoid colliding with obstacles and each ship. As there are commonly constrained terrains such as channel and canal in the ocean environment, moving ships in a formation will be adversely affected by the obstacles.

In addition, compared to mobile robots, unmanned aerial vehicles, unmanned ground vehicles, and autonomous underwater vehicles, resources of studies on formation control for unmanned surface ships are quite limited.

Therefore, this study intends contribute to a part of formation control, named coordinated path planning strategy for a fleet of multiple unmanned surface ships in the presence of static obstacles.

1.2. Motivation

Moving unmanned surface ships are critically influenced by bank, side-wall, and shallow water effects in the presence of static obstacles such as narrow channel between islands or lands.

Moreover, a fleet of ships in a formation is much more crucially influenced by the effects in the presence of the obstacles because of the number of ships and the size of formation shapes.

Therefore, this study focuses on change of the formation shapes to reduce influences of the effects in the presence of static obstacles without any collisions.

Figure 1.1 School of fish in a ball formation

The motivation of this study is from nature in the ocean. In Figure 1.1, there are a number of fish moving in a formation called a school of fish. The school of fish shapes their own formation and avoid gaps between large rocks with changing formation shape by natural instinct.

Accordingly, this study assumes that behaviours of the school of fish follow three rules:

1) There is a leader that decides directions and goal point for the group.

2) The rest of the schooling fish are followers that follow the leader in a pre-defined formation.

3) The formation shape of the group is changed into a safer formation shape when the school of fish face static obstacles.

The assumptions from the motivation gives solutions and insights to the problems of coordinated path planning for a fleet of unmanned surface ships in the presence of static obstacles. These assumptions are extended to three main parts of this study:

1) Path planning for a leader

2) Formation control

3) Coordinated path planning strategy

1.3. Aim and objectives

The overall aim of this research is to contribute to the realisation of unmanned navigation. The aim is to develop strategies for a fleet of unmanned surface ships to avoid static obstacles. More specific objectives are as follows:

a) To review the state-of-the-art techniques for path planning, formation control and coordinated path planning.

b) To devise a strategy of coordinated path planning based on three behavioural assumptions.
c) To investigate the feasibility and efficiency of the devised strategy in various navigational circumstances.
d) To put forward ideas on how to apply the strategy to the autonomous navigation of a fleet of unmanned ships.

1.4. Approach

This chapter introduces a process of how to achieve the aim of the research. The approach can be summarised in four tasks as follows:

a) Review various published material dealing with path planning, formation control and coordinated path planning to identify suitable algorithms to apply to the case of fleets of multiple surface ships.
b) Devise a strategy to integrate the identified algorithms for coordinated path planning.
c) Implement the proposed strategy in MATLAB/Simulink environment to create a simulation tool.
d) Carry out a parametric study to investigate the efficiency and the feasibility of the strategy.
e) Discuss the simulation results.
f) Put forward recommendations for future work.

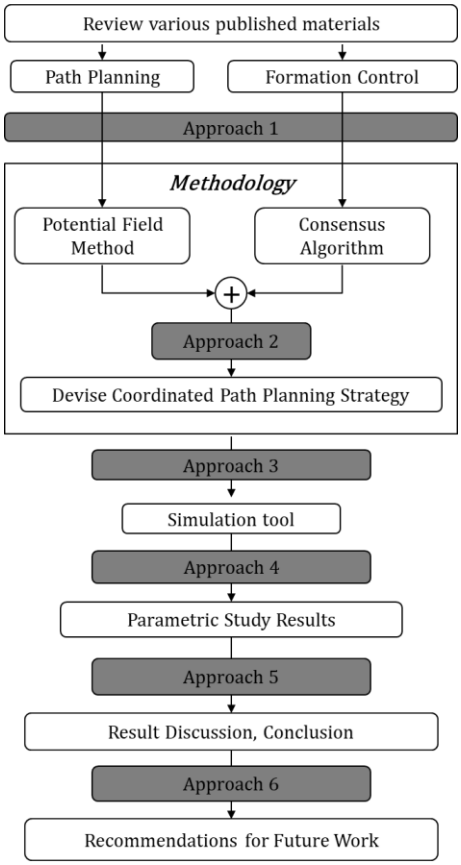

Figure 1.2 Flow-chart of the approach

The flow of the approach in this study is described in Figure 1.2.

1.5. Layout of Thesis

This thesis consists of five chapters and five appendices, each of which covers the following contents:

Chapter 2 is the literature review to provide the state-of-the-art in formation control, coordinated path planning for marine ships, aerial vehicles and ground vehicles.

Chapter 3 is the methodology that defines three problems with planning a coordinated path in the ocean environment with static obstacles.

Chapter 4 is the simulation part to validate the methodology by using the MATLAB environment.

Chapter 5 is to discuss the simulation results, to conclude and to put forward future work

Appendix A, Appendix B, Appendix C are to give better understanding for readers about formation control.

Appendix D is a part of simulation results on case 2.

Lastly, Appendix E is the MATLAB code of the proposed methodology

Chapter 2. Literature review

The drive towards a system of unmanned autonomous vehicles has resulted in a variety of research publications into the development of coordinated path planning for multiple vehicles that can promote the system more effectively and cooperatively.

The purpose of this chapter is to provide an overview of the recent research in formation control, especially coordinated path planning for marine ships. However, due to limited research studies on coordinated path planning for multiple unmanned surface ships, literature from not only unmanned ships but also mobile robots, unmanned aerial vehicles (UAV), unmanned ground vehicles (UGV), and unmanned underwater vehicles (UUV) has been reviewed.

2.1. Overview of formation control

The fields of formation control as well as coordinated path planning started to be investigated in the late of 1980s by several researchers who were interested in multiple vehicles systems (Parker 2000). Therefore, there have been numerous review and survey papers for formation control (Chen, Wang 2005),(Murray 2007), (Campbell, Naeem et al. 2012), (Parker 2000), (Kanjanawanishkul 2016), (Cao, Fukunaga et al. 1997) and (Hernández-Martínez, Aranda-Bricaire 2011). The review papers in the above provide valuable information on current research topics, definition, practical problems, and solutions of cooperative formation control in multiple vehicle systems.

Parker, (2000) stated distributed autonomous multi-robot systems focused on physical robot implementations. He divided research topics on multi-robot systems into eight primary parts:

A. 'Biological inspirations' that give strong influence on cooperative mobile robotics research because 'Biological inspirations' are the root of behaviour-based control that is the first paradigm of cooperative mobile robotics.

B. 'Communication' in multiple robots to convey information to robot members of the team.
C. 'Architectures, Task planning and Control' has been researched because it gives a great advantage to enable robots to achieve *task planning, fault tolerance, swarm control, human design of mission plans*.

D. 'Localization/Mapping/Exploration'. Recently, amount of studies on multiple robots have been researched to enhance positioning accuracy for a team of robots.

E. 'Object transport and manipulation' has been researched to enable multiple robots to cooperatively carry, push, or manipulate common objects.

F. 'Motion coordination' is popular topic in this area, where it includes the studies of *multi-robot path planning, traffic control, formation generation, and formation keeping***.**

G. Relatively a few researches of ***'Reconfigurable robots'*** has been carried out. However, 'Reconfigurable robots' is important topic in that it is to achieve generation of a desired shape.

H. 'Learning' is a challenging and potential area in multi robot systems to solve complex cooperative tasks such as *predator/prey, box pushing, foraging, and multi-robot soccer*.

Compared with Parker, (2000), Kanjanawanishkul , (2016) reviewed formation control of ground mobile robotics in a similar way but the paper classified formation control as four problems:

A. 'Formation shape generation' that focuses on how to form and how to maintain a formation

B. 'Formation reconfiguration and selection' that is necessary to switch/change/split/join the formation due to change in environment's configuration such as narrow corridors

C. 'Formation tracking' that is the biggest part of formation control research. The objective of 'Formation tracking' is to enable a group of robots to maintain a desired formation while tracking a reference

D. 'Role assignment in formation' that is to achieve an assignment of the robots in a desired formation

The main technical approaches on the formation control problems were summarized in Murray, (2007). The approaches were categorized in four parts:

A. 'Formation control' to maintain a desired formation shape

B. 'Cooperative tasking' to satisfy a group objective

C. 'Spatial-temporal planning' to generate paths of the robots

D. 'Consensus algorithms' to reach a common decision based on distributed information. Similarly, Cao, (1997)argued that because multiple mobile robots must interact with each robot physically, ***'Geometric issues'*** that include (multiple-robot) path planning, moving to formation, maintaining formation and pattern generation are regarded as inherent problems of multiple-robot systems in the cooperative robotics.

With respect to formation control, Chen, (2005) described current formation control issues and formation control strategies on a group of unmanned autonomous vehicles. The control strategies are divided into four approaches in the paper:

A. 'Behaviour-based approach and potential field approach' that generates a vector to represent the desired behaviour response

B. 'Leader-follower approach', where leader tracks a predefined path and followers maintain a desired separation with the leader

C. 'Generalized coordinates approach' that characterize the vehicle's location, orientation, and its shape with respect to a reference point in the formation

D. 'Virtual structure method' to force a team of vehicles to behave in a rigid formation.

The summary of formation control review papers is described in Figure 2.1.

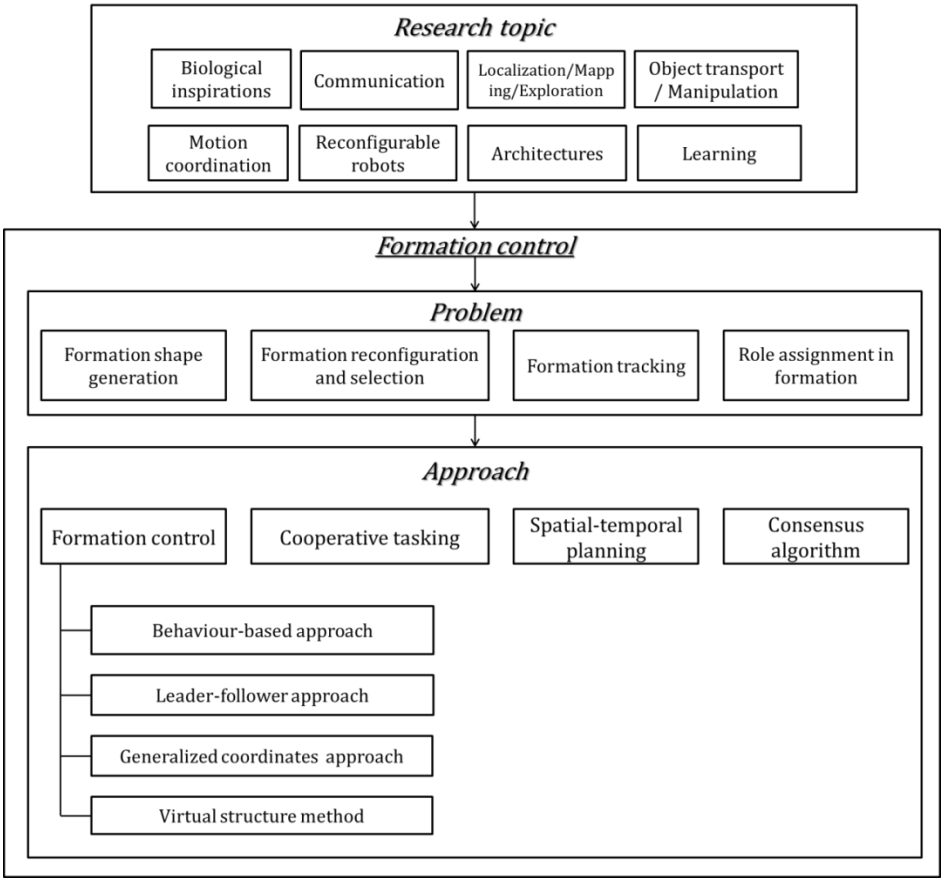

Figure 2.1 Overview of formation control

2.2. Formation control approaches in the presence of obstacles

As mentioned in section 2.1, the geometric issues on formation control are a critical challenge to solve in the existence of static and dynamic obstacles. There have been a great number of studies on avoiding hazard obstacles and maintaining a formation at the same time for a team of unmanned vehicles.

Firstly, a behaviour-based approach to robot formation-keeping is proposed in Balch, (1998). In the article, formation and navigational behaviours are integrated to achieve navigational goals, avoid hazards, and keep formation simultaneously. In addition, several motor schemes designated as move-to-goal, avoid-static-obstacle, avoid-robot and maintain-formation enables robots to move to a goal while avoiding obstacles without collision with other robots and remaining in formation. The results of a motor scheme-based formation control in simulation were generated in the presence of static obstacles with quantitative differences between formation types and references. Contemporarily, Desai, (1998) presented feedback laws to control multiple robots moving together in a formation in an obstacle environment by using only local sensor-based information and a leader-follower approach. The simulation implementations of the feedback laws for multiple robots were shown in two formation cases, moving in constant formation and change in formation with static obstacles in the environment. Even if the result of simulation in a case of '*constant formation'* shows that one or all of group members move slightly to avoid obstacles in a constant formation shape, the result in a case of

'change in formation' displays changing triangle formation shape to rectangle formation to avoid the obstacles not recovering rectangle formation to the original formation shape.

Recently, a solution of formation stabilization and tracking for a group of mobile robots by using virtual force method to avoid obstacles and leader-follower approach was proposed by Mohammadi, (2013). Simulation results of the solution demonstrate that a group of mobile robots change direction and keep formation with static obstacles in the map at the same time. An optimal path solution using Asexual Reproduction Optimization (ARO) that has a remarkable fast convergence time for mobile robots in a leader-follower structure was presented by Asl, (2014). Simulation results of the optimal path planning for mobile robots show that a group of the robots maintain formation when they are not close to obstacles and the formation does not occur when followers are close to the obstacles.

In terms of formation control for a fleet of marine vehicles in the presence of obstacles, Campbell, (2012) argued that it is a more difficult and challenging topic due to the complex nature and relation to the International Regulations for Avoiding Collisions at Sea (COLREGs). In addition, Campbell, (2012) suggests that the purpose of formation control for a fleet is to navigate to a goal location, whilst keeping a formation pattern and successfully avoiding obstacles.

Arrichiello, (2006) applied ***'Null-space-Based behavioural control' (NSB)*** to a fleet of marine surface vessels to perform multiple tasks such as obstacle avoidance or keeping a formation in complex environments by selecting dynamically the motion reference commands for each vessel. To verify the algorithm, two cases of simulations are implemented. A fleet of vessels can pass safely in both situations of bottle neck obstacles and randomly positioned obstacles in the presence of environmental disturbances. Furthermore, Arrichiello, (2006) argues that the algorithm can allow changing formations to overtake the obstacles, for example, it can be change a V shaped formation into a line formation to pass the obstacles and it would be reshaped to the desired configuration when the fleet is far from the obstacles. However, simulation result of the argument is not shown in the paper.

Recently, Liu, (2015) proposed path planning algorithm by using the fast marching (FM) method to enable to model the dynamic behaviour of moving ships with reasonable computation time. Owing to high uncertainty and complexity of obstacles in a real ocean environment, it is primary to consider safety of a fleet of ships. Therefore, Liu, (2015) devises sufficient safe distance to be maintained between ship and static obstacles as well as dynamic obstacles. To create collision free path in real time, Liu, (2015) adopts leader-follower structure along with the real time path planning scheme to maintain formation shape. To evaluate the algorithm, two simulation tests have been carried out in dynamic environment with moving obstacles. When the fleet manoeuvres in a narrow channel, the fleet in a triangle formation can avoid successfully the channel and moving ships by forming into a line formation. However, it does not show reshaping into the original formation, line formation, after passing through the channel. Following from this work, the author proposed the angle guidance formation path planning algorithms using the FM method named ***'angle-guidance fast marching square' (AFMS)*** to create path compliance with vehicle's dynamics and orientation limit in a cluttered

environment (Liu, 2016). The algorithm enables the unmanned surface vehicles (USVs) to form a desired shape by following the trajectory from random initial positions and orientations. In addition, the distance to the closest point of approaching (DCPA) concept is used in order to reduce the potential collision risks. To validate the algorithm, Liu, (2016) implemented two sets of simulation, where the both tests are to carry out formation path planning algorithm for a fleet of USVs depending on heading angles in different static environment condition. The fleet of USVs in a constant formation can successfully reach a goal position without any collisions in a cluttered environment.

Similar with USVs, many studies of formation control for autonomous underwater vehicles (AUVs) in an environment with obstacles have been researched. Yang, (2011) presented a motion planning algorithm for multi AUVs formation in the presence of static obstacles by using artificial potential field (APF) and Kane's method (Bajodah, 2003). Particularly, APF is used to formation motion control for mission requirement, environment, and formation configuration. In addition, the integrated algorithm of APF and Kane's method gives an advantage which coordinated control and formation motion planning can be operated at the same time. To validate the integrated methodology, simulations for AUVs formation is implemented in three-dimensional space with a sphere obstacle. The AUVs were modelled as a set of point masses with full actuation move to the goal point in a constant formation whilst avoiding the static obstacle. However, it is necessary to consider more complex obstacles for verifying that the AUVs formation can be maintained and move safely to the goal point in the complex environment.

Similarly, Hou, (2008) proposed an *intelligent behaviour-based team unmanned underwater vehicles (UUVs) cooperation and navigation in a water flow environment with obstacles*. The concepts of the algorithm come from group animal behaviour and Hou, (2008) developed the five behaviour-based rules for UUVs formation by using fuzzy logic. To verify the behaviour-based algorithm, real dynamic UUV model is used in simulations. The simulation results show the UUVs' trajectories in a current environmental disturbance with static obstacles. As relatively a few studies consider environmental disturbances in ocean with static obstacles, the contribution of Hou, (2008) would give positive impacts on cooperative control for unmanned marine vehicles. However, the movement of a fleet of UUVs in this simulation is oscillated around obstacles and between obstacles.

2.3. Coordinated formation strategies in the presence of static obstacles

As reviewed in section 2.2, there have been several research studies on formation control in the ocean environment with obstacles. However, a problem of the formation control is found. Arrichiello, (2006), Desai, (1998), and Liu, (2015) did not show that a group of vehicles is not reshaped into original formation shape after avoiding static obstacles. In this section, therefore, this thesis reviews coordinated formation approaches for multi vehicles in the presence of the obstacles, such as formation selection, formation changing, formation switching and formation reconfiguration (Chen, 2008), (Fan, 2010), (Radovnikovich, 2014) and (Dai, 2015).

Chen, (2008) designed a decentralized formation controller that consists of two parts, formation description and formation control using an adaptive neural network (ANN). To analyse the stability of the proposed formation control algorithm when formation pattern and interaction topology are variant, simulation based on particle swarm optimization (PSO) is implemented. In a simulation, two formation patterns are applied: a triangular formation and a line formation. When the leader perceives obstacles, a group of robots changes their triangle formation pattern to a line formation pattern to avoid obstacles without collision. As a result, the group of robots can form the triangular formation shape from randomly initial positions, and the group passes through complex obstacles as changing their formation into the line pattern. In addition, the group reshapes to the original formation pattern after passing all obstacles. However, the simulation result does not show detail descriptions of transition situation from the original formation to a new formation pattern when the group passes through the obstacles.

Similarly, collision free formation changing control algorithm was proposed by Fan, (2010). Formation changing rules are based upon sensor information. In addition, artificial potential method and control matrix are used to reconfigure formations. In order to verify the algorithm, simulations for eight AUVs under complex environment are performed. The simulation result shows that the swarm of AUVs successfully moves through the constrained environment as the formation shape changes from the original formation to a final formation shape by three times. However, Fan, (2010) considered the case of changing formation pattern when only two or more AUVs are in danger.

Radovnikovich, (2014) proposed an interesting topic on an optimal planning algorithm for multi vehicles to avoid tunnel type obstacles by a breaking formation pattern and recombining into the original formation. Lyapunov's direct method is used to control formation and fuzzy logic is utilized to avoid the obstacles. To validate the feasibility of the algorithm, an experiment for multiple vehicles is implemented in the case of passing through a tunnel. The experiment results show successful collision free formation control. Formation of the vehicles is rigidly constructed at first before facing the tunnel. As the follower vehicles perceive the tunnel, the formation is broken to avoid collisions with the tunnel wall and the size of the formation is shrunk to get through the narrow tunnel. After negotiating the tunnel, the original formation is reshaped. Even though the experiment proves the formation breaking strategy enables the group of vehicles to avoid both side obstacles such as tunnel and narrow corridor, the result does not show whether one side of the formation would be broken or both wings of the formation would be broken in the presence of one sided obstacles. When the both sides of the formation are broken, it would give negative impacts on the efficiency of formation navigation.

Recently, Dai, (2015) investigated a switching formation strategy for multi-robots to avoid and pass obstacles by using geometric obstacle avoidance control method (GOACM). The strategy makes leader robot plan a safe path using the method and follower robots switch into a safe formation by calculating desired distances and angles with the leader. In addition, in order to avoid obstacles a novel robot priority model is designed. In terms of demonstrating validity of the proposed algorithm, both of simulation and experiment are implemented. The simulation result shows the team of multi-robots crosses tunnel type obstacles and avoids one side obstacle.

In addition, the team switch the predefined formation to safe formations such as a line and triangle formation and switch back into the original formation pattern. With respect to switching algorithm, however, position errors of the leader and the followers change suddenly now that the robots determine to switch formation pattern. The errors might cause negative behaviours for controlling multi-robots.

In conclusion, this section provided the overview of the recent research in formation control to understand the general background of formation control. In addition, this section reviewed papers on approaches for the geometric problems on formation control in the presence of obstacles for multi vehicles to consider avoiding the obstacles and keeping a formation at the same time. Finally, this section investigated coordinated formation control strategies that are reshaped into the original formation shape after passing through static obstacles by using several strategies, formation selection, formation changing, formation switching, and formation reconfiguration.

From the literature review, this research study on coordinated path planning strategy was motivated by ***'Biological inspirations'***. In addition, the study dealt with the problem of ***'Formation reconfiguration and selection'*** by using approaches of ***'Spatial-temporal planning'*** and ***'formation control'*** based on ***'Leader-follower approach'*** to avoid static obstacles.

Chapter 3. Methodology

This chapter defines three problems with planning a coordinated path in the ocean environment with static obstacles. In addition, this chapter solves the problems and propose a new strategy. This chapter describes the problems and solutions in Figure 3.1.

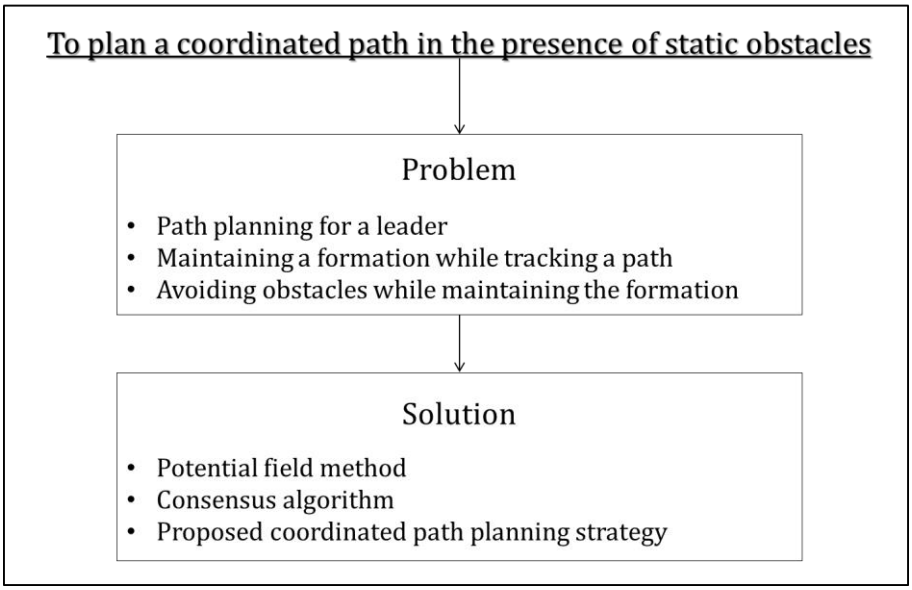

Figure 3.1 Definition of problems and solutions

To plan a path for a fleet of unmanned surface ships, this chapter considers planning a path for a leader, maintaining a formation and avoiding obstacles. this study uses the potential field method (PFM) for a path planning, consensus algorithm for formation control, and propose a new path planning strategy for a fleet to avoid static obstacles.

Therefore, the methodology for coordinated path planning in the presence of the obstacles is organized into three sections: 1. Path planning for a leader, 2. Formation control, 3. Coordinated path planning strategy.

3.1. Path planning for a leader

This section the PFM, gradient descent and examples of path planning for one single leader ship. PFM can represent a given map of vectors that are the sum of attractive vectors by a goal and repulsive vectors by static obstacles. Therefore, a leader is influenced to pull from a goal and to push away from the obstacles. Gradient descent is an optimization method to find a minimum value. Therefore, the leader can plan a path from a start point to minimum value called a goal point by using the PFM and gradient descent.

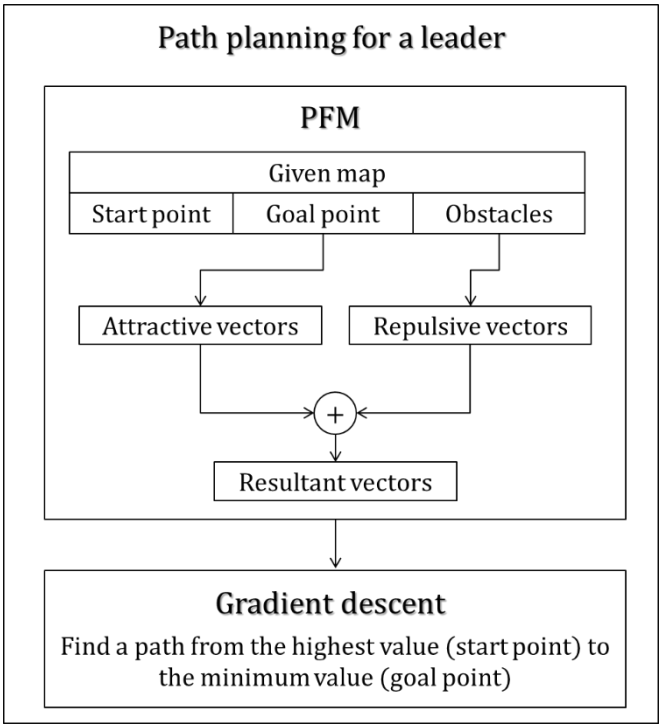

Figure 3.2 flow of path planning using PFM and gradient descent

Figure 3.2 shows the process of path planning for a leader. Firstly, a given map consists of a start point, a goal point and obstacles. The sum of two types of vectors generates vector field in the given map. Finally, a path can be planned by converging towards the smallest value of gradient from start point.

3.1.1. Potential field method (PFM)

PFM is frequently used in path planning algorithm because there are a number of advantages such as highly safe, mathematically simple and elegant (Cen, Wang et al. 2007). The basic idea of PFM is to fill a two-dimensional map with an artificial potential vector field where the vehicle can be attracted to the goal position and can be repulsed away from the obstacles.

PFM uses a scalar function called a potential function. The potential function consists of attractive potential function and repulsive potential function. Firstly, the attractive potential function is defined as a function of a relative distance between the goal point and a vehicle in the map(Ge, Cui 2002). Secondly, the repulsive potential function is defined as a relative distance between obstacles and the vehicle(Pradhan, Parhi et al. 2006). In addition, resultant potential function is sum of the attractive potential function and the repulsive potential function. To simplify the path planning using the PFM, two assumptions are required. The first assumption is that the vehicle is assumed as a point mass and the second is that the vehicle moves in a two dimensional map (Pradhan, Parhi et al. 2006).

Attractive potential function

The attractive potential function $U_{att}(q)$ can be defined by Ge, Cui (2002) in the below equations.

$$U_{att}(q) = \frac{1}{2} k_{att} \rho_{goal}(q)^2 \tag{3.1}$$

$$\rho_{goal}(q) = \left\| q - q_{goal} \right\| \tag{3.2}$$

$$q = [x, y] \tag{3.3}$$

Where k_{att} is a positive scaling factor, $\rho_{goal}(q)$ denotes the Euclidean distance between the vehicle position q and the goal position q_{goal} in a two dimensional map.

Attractive potential force generated by the goal is given by the negative gradient of the attractive potential function(Ge, Cui 2002).

$$F_{att}(q) = -\nabla U_{att}(q) = -k_{att} \cdot \rho_{goal}(q) \nabla \rho_{goal}(q) = -k_{att} \cdot (q - q_{goal}) \tag{3.4}$$

$$\nabla = \frac{\partial}{\partial x} i + \frac{\partial}{\partial y} j + \frac{\partial}{\partial z} \hat{k} \tag{3.5}$$

For example, as the vehicle position q goes into q_{goal}, $F_{att}(q)$ converges towards zero because the distance between q and q_{goal} is gradually close to zero. Figure 3.3 shows the attractive potential force between q and q_{goal}.

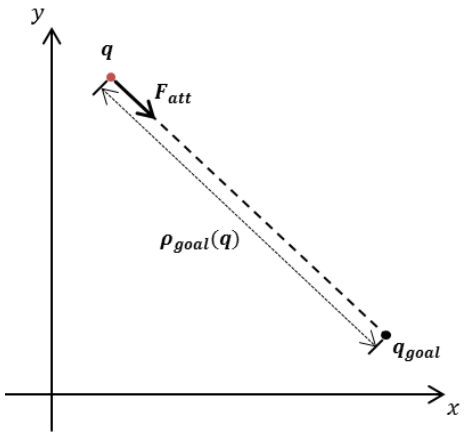

Figure 3.3 The attractive potential force in a two dimensional space

Repulsive potential function

The repulsive potential function $U_{rep}(q)$ is given by Ge, Cui, (2002) in the below equation.

$$U_{rep}(q) = \begin{cases} \frac{1}{2} k_{rep} (1/\rho(q) - 1/\rho_0)^2 & if\ \rho(q) \le \rho_0 \\ 0 & if\ \rho(q) > 0 \end{cases} \tag{3.6}$$

Where k_{rep} is a positive scaling factor, $\rho(q)$ is the minimum distance between the vehicle position q and the obstacle. In addition, ρ_0 is a constant value that represents distance of

influence of the obstacles. As the vehicle position q is getting closer to the obstacle, the repulsive potential function $U_{rep}(q)$ is increasing to infinity.

The repulsive potential force generated by the obstacles and the influence of the obstacles is described by the negative gradient of the repulsive potential function in (5.7), Figure 3.4(Ge, Cui 2002).

$$F_{rep}(q) = -\nabla U_{rep}(q) \tag{3.7}$$

$$= \begin{cases} k_{rep}(1/\rho(q) - 1/\rho_0) \cdot 1/\rho^2(q) \cdot (q - q_{obs})/\rho(q) & if\ \rho(q) \le \rho_0 \\ 0 & if\ \rho(q) > 0 \end{cases}$$

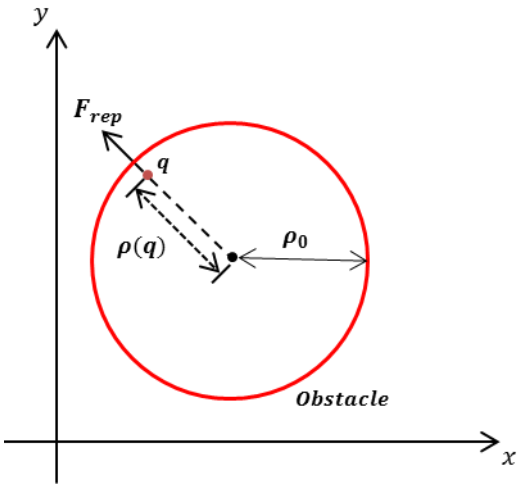

Figure 3.4 The repulsive potential force

If there are n obstacles in a map, the total repulsive potential force is obtained by (3.8).

$$F_{rep} = \sum_{i=1}^{n_{obs}} F_{rep_i} \tag{3.8}$$

Where n_{obs} is the number of obstacles and F_{rep_i} is the repulsive force obtained by the i^{th} obstacle. After calculating the attractive force and the repulsive force, finally, resultant potential force can be obtained in (3.9) (Ge, Cui 2002).

$$F_{total} = F_{att} + F_{rep} \tag{3.9}$$

The resultant potential force F_{total} imposing on a point mass vehicle tends to go toward the goal and push away from the obstacles.

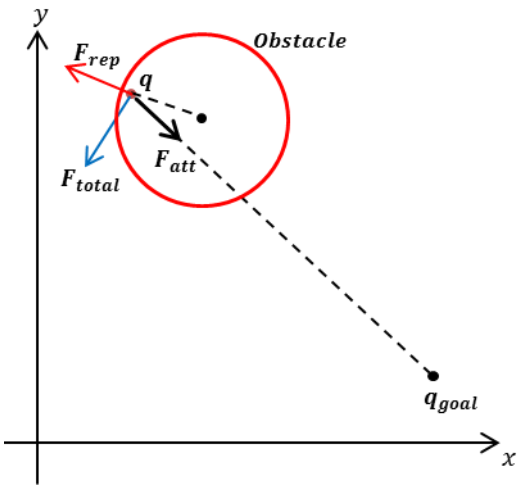

Figure 3.5 The resultant potential force

Figure 3.5 shows the repulsive potential force as a red arrow, the attractive potential force as a black arrow and the total potential as a blue one.

3.1.2. Gradient descent

Gradient descent is a popular optimization algorithm that minimizes a gradient at a point. The basic idea of gradient descent can be simply defined. As a calculation of gradient descent starts at a start point, it takes one step proportional to the negative gradient. A new point is obtained by calculus, and the repeated process is performed until the gradient reaches to the minimum value (Choset 2005).

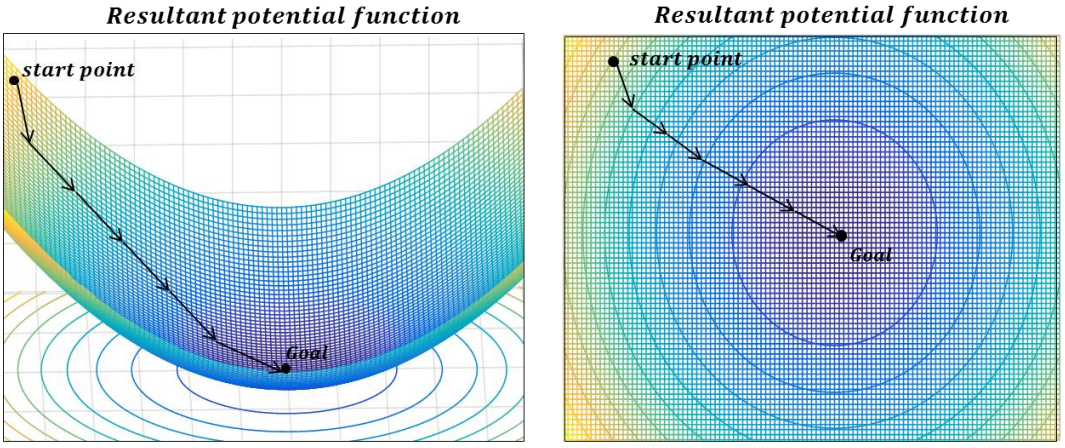

Figure 3.6 Find a path by using gradient descent from start point

Figure 3.6 shows a path planning using gradient descent in a resultant potential function field. The point mass vehicle tends to move to a lower potential function until the potential function is minimized at the vehicle position. Therefore a path can be obtained as well as a direction and magnitude information of the vectors from the start point to the goal point.

3.1.3. Example

An example shows the entire process of path planning by using PFM and gradient descent in MATLAB/Simulink environment. The process of path planning is defined by five steps described in the below.

a) : Drawing a binary map

b) : Obtaining an attractive potential function

c) : Obtaining a repulsive potential function

d) : Calculating a resultant potential function

e) : Planning a path by using gradient descent

Figure 3.7 Customized map

Figure 3.7 shows a customized map that represents a complex confined waterway. In Figure 3.7, the map consists of two spaces, the first space is a black part that depicts obstacles such as land and island. The second space is white part that describes sea as a free space. In addition, start point located in left-upper side and goal point placed in right-lower are designated on the map.

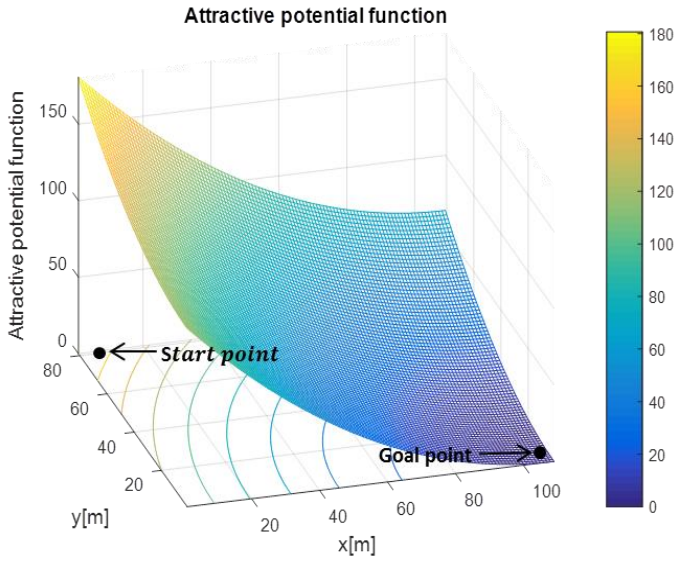

Figure 3.8 Attractive potential function for the map

Figure 3.8 is a three-dimensional representation of an attractive potential function in the map. The xy plane represents the horizontal plane of the map and the z-axis represents an attractive potential function. The colour bar represents the strength of the attractive potential function that the larger strength has more yellow and the smaller strength represents purple. In Figure 3.8, two points that represent start point (x, y) and goal point (x_{goal}, y_{goal}) located at (1,80) and (109,1), respectively.

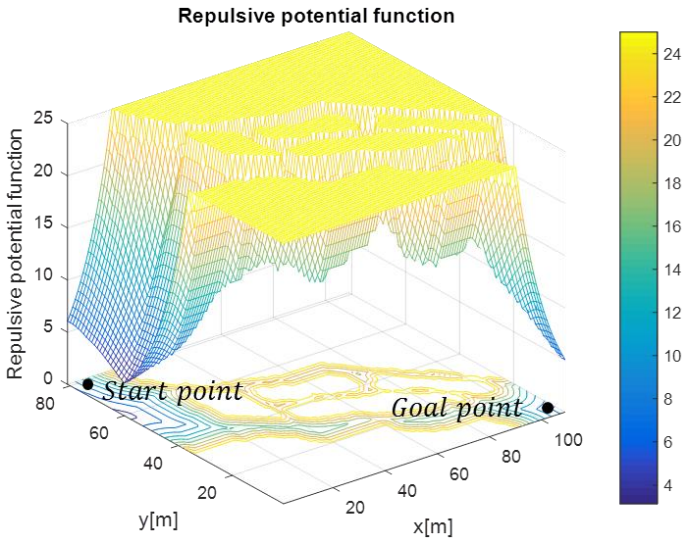

Figure 3.9 Repulsive potential function for the map

Figure 3.9 shows the repulsive potential function in three-dimensional map. Compared with Figure 3.7 and Figure 3.9, the black space that represents static obstacles in Figure 3.7 indicates to yellow flat part in Figure 3.9. As shown in Figure 3.9, the area of obstacles in the map has the highest strength of the repulsive potential function. On the other hand, the repulsive potential function is less strong in the free space.

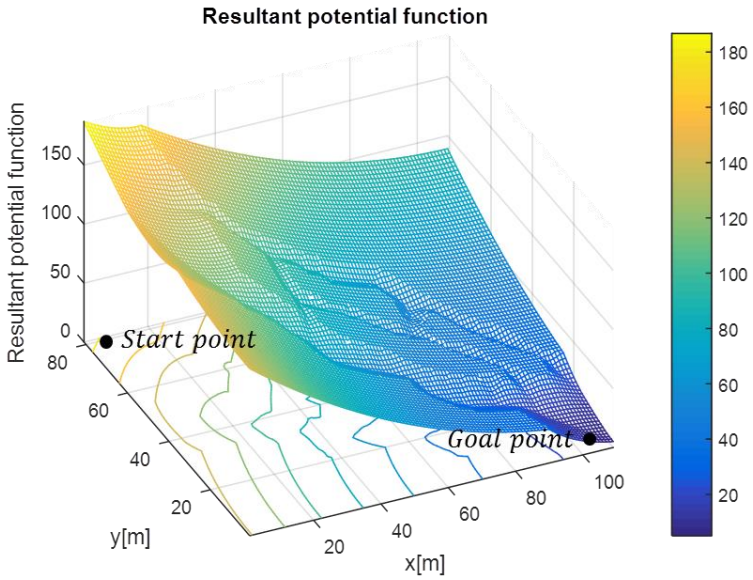

Figure 3.10 Resultant potential function for the map

Figure 3.10 shows the resultant potential function that is sum of attractive potential function and repulsive potential function. Therefore, the resultant potential function has the highest strength at the start point, and the lowest strength at the goal point.

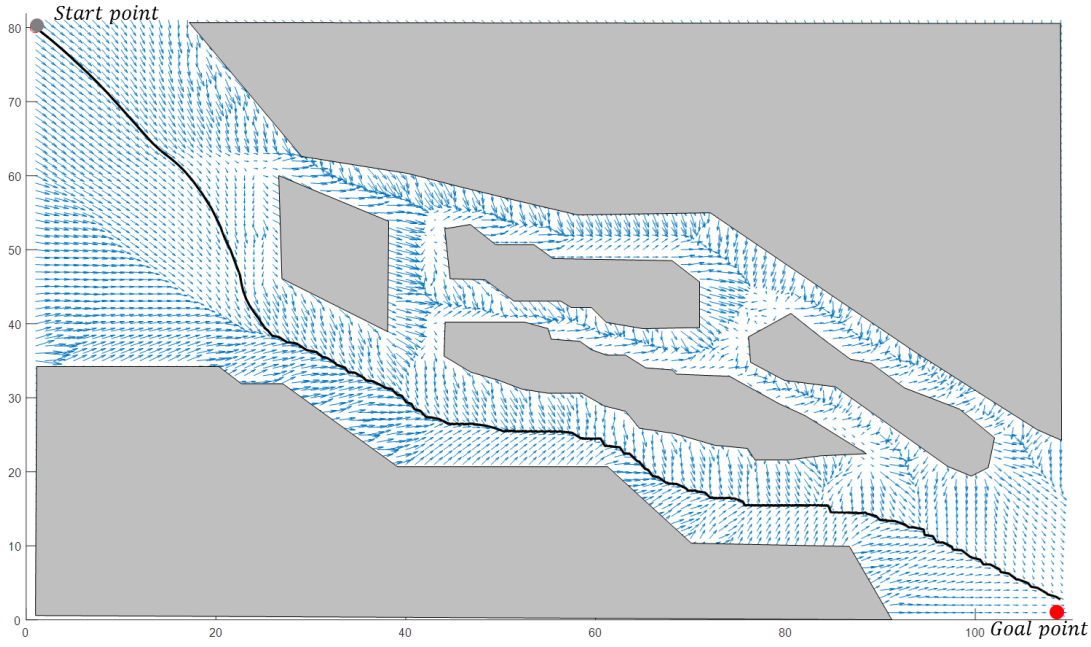

Figure 3.11 Path planning using gradient descent

In Figure 3.11, a black solid line indicates a path planned by using gradient descent from the start point to the goal point and grey shapes represent static obstacles. Blue arrows are vectors that show the direction and the magnitude of gradient of the resultant potential function. At the start point, the direction of the vectors is around the goal point because there is not the influence of the static obstacles. However, the direction of the vectors near the obstacles is tilted to the outside of the obstacles because the vector is affected by the obstacles. At x= 25, the reason

why the path goes to wide channel not to narrow channel is because the magnitude of the gradient near wide channel is higher than near narrow channel.

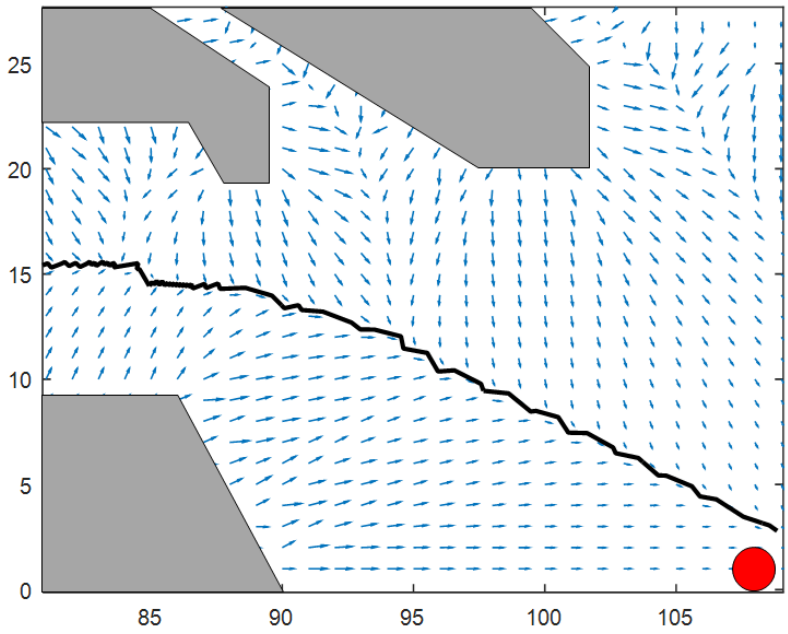

Figure 3.12 Enlarged map at the goal point

At the goal point, the black solid line cannot reach the goal point exactly because of a characteristic of a numerical simulation, therefore, path planning is terminated when the distance between the point mass vehicle and the goal point is less than 2.0 $[m]$. In conclusion, as shown in Figure 3.11 and Figure 3.12, a safe path that has tendency to reach the goal and move away from the obstacles is planned in the map

However, the path has oscillation in the narrow channel because of an inherent drawback of the PFM(Koren, Borenstein 1991). To overcome the drawback, one of path smoothing algorithms that pick way-points on the path is used and each way-point is connected with lines by using 'cubic Hermite interpolation'.

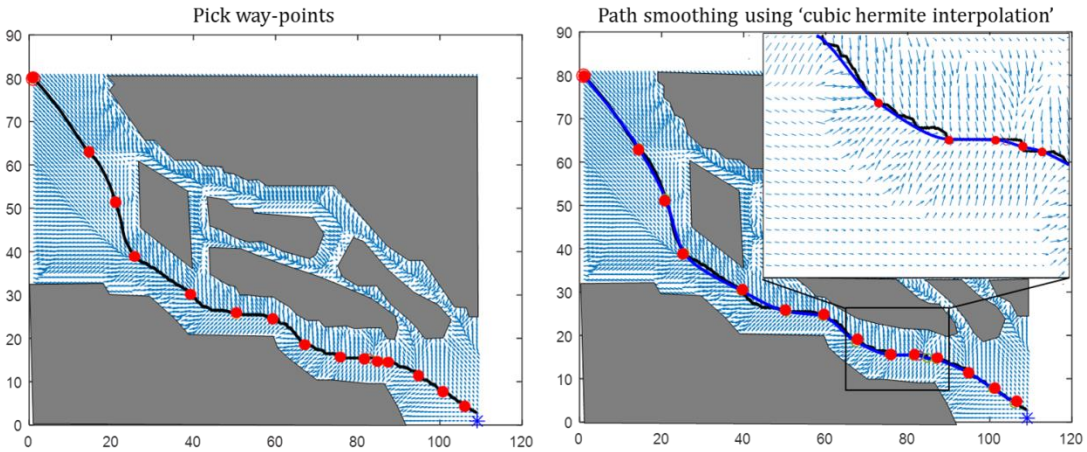

Figure 3.13 Path smoothing

Figure 3.13 shows picking way-points represented as red points and a smoothed path described as a blue line. In addition, Figure 3.13 shows an enlarged description of the smoothed path, where the black oscillated line is smoothened in the narrow channel.

3.2. Formation control

In order to form a pre-defined formation shape and track a planned path in the formation, a fleet of unmanned surface ships should share their position information with each ship to reach a cooperative agreement. To achieve the aim, in this study, a consensus algorithm is selected for formation control of a fleet.

3.2.1. Consensus algorithm

This section introduces an equation of formation control based on the consensus algorithm and show a comprehensive example of application to a fleet of the ships.

Suppose that there are n ships in a fleet. To represent communication environment with each ship, directed graph $G_n \triangleq (V_n, E_n)$ is used, where $V_n = \{1,\ldots,n\}$ is node set and $E_n \subset V_n \times V_n$ is edge set. Let $A_n = [a_{i,j}] \in \mathbb{R}^{n\times n}$ be adjacency matrix related with G_n (see Appendix A for graph theory notations).

This study assumes that unmanned surface ships are modelled as point mass models. Dynamics of point mass models is given by $\dot{x}_i = u_i, \quad i = 1,\ldots,n$, where $x_i \in \mathbb{R}$ is information state that indicates position and heading angle of ships in addition, $u_i \in \mathbb{R}$ is control input of ith ship.

Furthermore, a fundamental consensus algorithm is given by $u_i = -\sum_{j=1}^{n} a_{ij}(x_i - x_j), \quad i = 1,\ldots,n$

where a_{ij} is the (i, j) element of the adjacency matrix A_n (see Appendix B for fundamental consensus algorithm).

The *fundamental consensus algorithm* needs to be extended to *consensus tracking algorithm* with a leader because followers of a fleet should track a leader's path in a formation. In addition, a time-varying path is considered because the leader tracks not only a time invariant path but also a time-varying path in most path following situations (see Appendix C for extended consensus algorithm).

To build and keep formation for point mass models modelled by the dynamics, equation (C.1) and (C.2) are extended to an algorithm taking into account relative state deviations from a reference state.

The algorithm for relative state deviations from a time-varying reference state is written byRen, (2007a)

$$u_i = \dot{\delta}_i + \frac{1}{\eta_i}\sum_{j=1}^{n} a_{ij}\{\dot{\xi}_j - \dot{\delta}_j - [(\xi_i - \xi_j) - (\delta_i - \delta_j)]\} + \frac{1}{\eta_i} a_{i(n+1)}[\dot{\xi}^r - (\xi_i - \delta_i - \xi^r)] \qquad (3.10)$$

$\delta_i - \delta_j \triangleq \Delta_{ij}, \forall i \neq j$ means the desired separation between information states of neighbours. The control objective of the equation (3.10) is given by $\xi_i(t) \to \xi^r(t) + \delta_i(t)$ and

$\xi_i(t)-\xi_j(t)\to\Delta_{ij}(t)$, as $t\to\infty$, if and only if a graph G_{n+1} has a directed spanning tree structure.

An example describes equation (3.10) to track the relative deviation from time-varying reference. Initial condition of positions and a graph of five models are equal to condition of the previous simple scenario in addition, the reference state is $\xi_5=\xi^r(t)=\cos(t)$. Relative deviations from a reference state is given by $\delta_i=1-i$, $i=1,\ldots,4$.

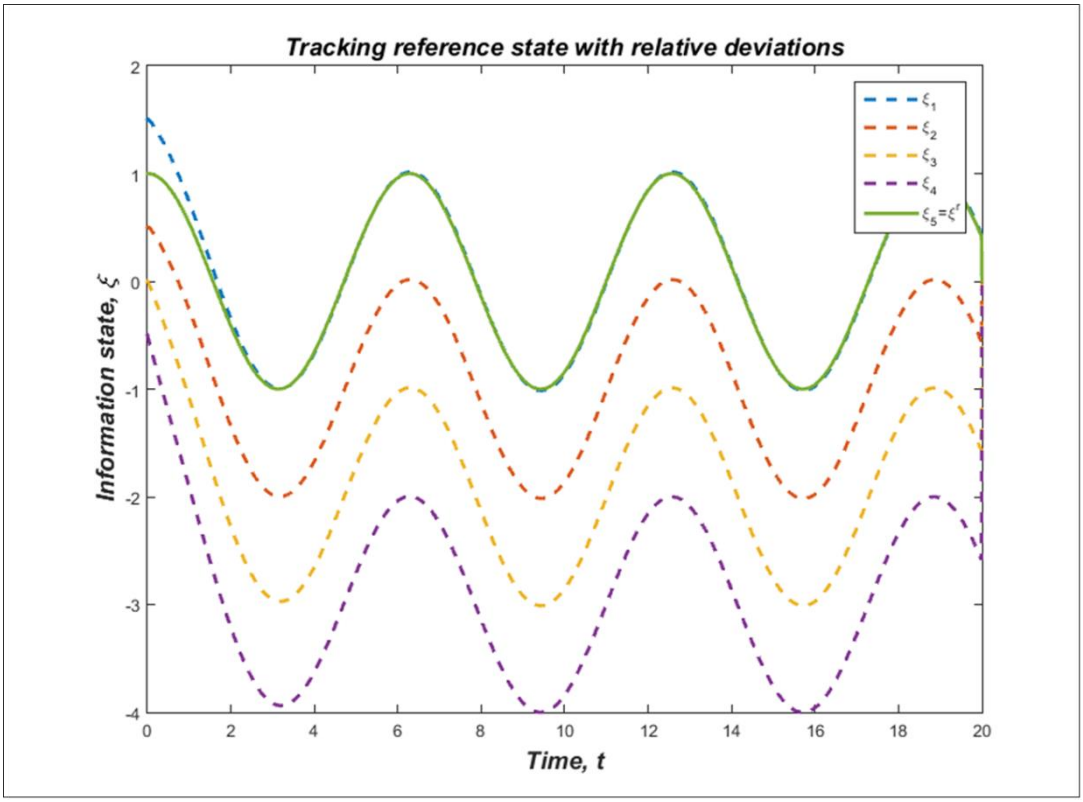

Figure 3.14 Information states of followers to track reference state with relative deviation

Where four followers and a leader are represented by dotted lines and a solid line, respectively. Figure 3.14 shows that $\xi_1(t)\to\cos(t)$, $\xi_2(t)\to\cos(t)-1$, $\xi_3(t)\to\cos(t)-2$ and $\xi_4(t)\to\cos(t)-3$ as $t\to\infty$.

3.2.2. Example

There is an example to keep a triangular formation for five models in two-dimensional space. In terms of two-dimensional space in equation (3.10), the control input, the deviations and the information states are defined by $u_i=[u_{xi},u_{yi}]^T$, $\delta_i=[\delta_{xi},\delta_{yi}]^T$ and $\xi_i=[\xi_{xi},\xi_{yi}]^T$ in two-dimensional space.

Firstly, the smoothened path is used in Figure 3.13. Initial positions of the five models are given by $(0,84)$, $(2,82)$, $(2,78)$, $(0,76)$ and $(4,80)$,respectively. The relative deviations of followers are set by $\delta_1=[-4,4]^T$, $\delta_2=[-2,2]^T$, $\delta_3=[-2,-2]^T$, $\delta_4=[-4,-4]^T$ and $\delta_5=[0,0]^T$.

The desired formation shape is a triangular geometry and described in below figure.

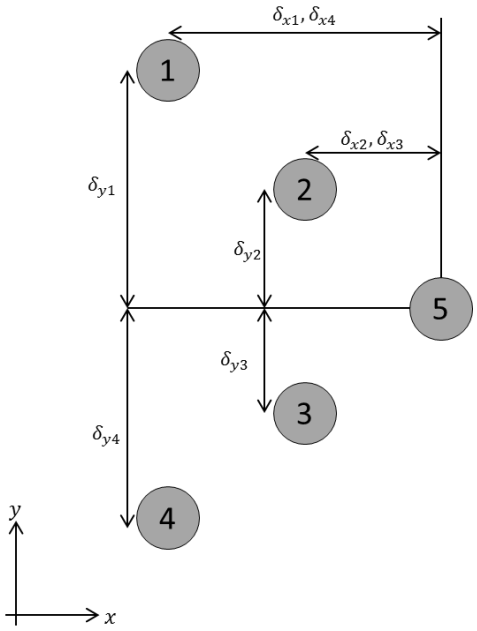

Figure 3.15 Triangular formation shape for five models

In addition, an adjacency matrix of a strongly connected graph is written in equation (3.11).

$$A = \begin{bmatrix} 0 & 0 & 1 & 0 & 1 \\ 0 & 0 & 1 & 0 & 1 \\ 0 & 1 & 0 & 0 & 1 \\ 1 & 0 & 0 & 0 & 1 \\ 0 & 0 & 0 & 0 & 0 \end{bmatrix} \tag{3.11}$$

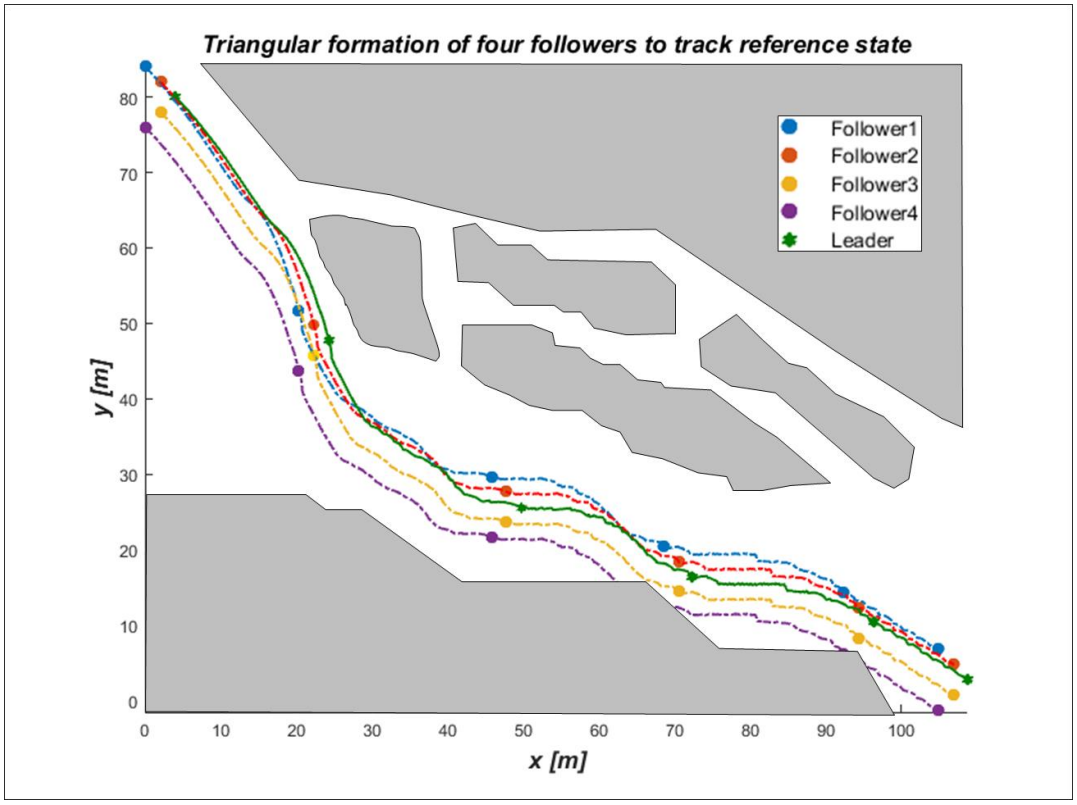

Figure 3.16 Four followers to track a leader with keeping formation

As shown in Figure 3.16, the map shows narrow channel and the planned path is designated as a reference state that a leader tracks. A formation of a fleet is a triangular shape at the start point, in addition, start point and goal point of the leader are $(4,80)$ and $(108,1)$.

Paths of four followers and a leader are represented as dotted lines and a solid line, respectively. The Paths of followers is generated safely until $x = 60[m]$, however the below follower 4 cannot avoid a static obstacles at approximately $x = 65[m]$ and $x = 95[m]$.

3.3. Coordinated path planning strategy

Figure 3.17 shows an enlarged Figure 3.16 and describes a collision situation between static obstacles and a follower.

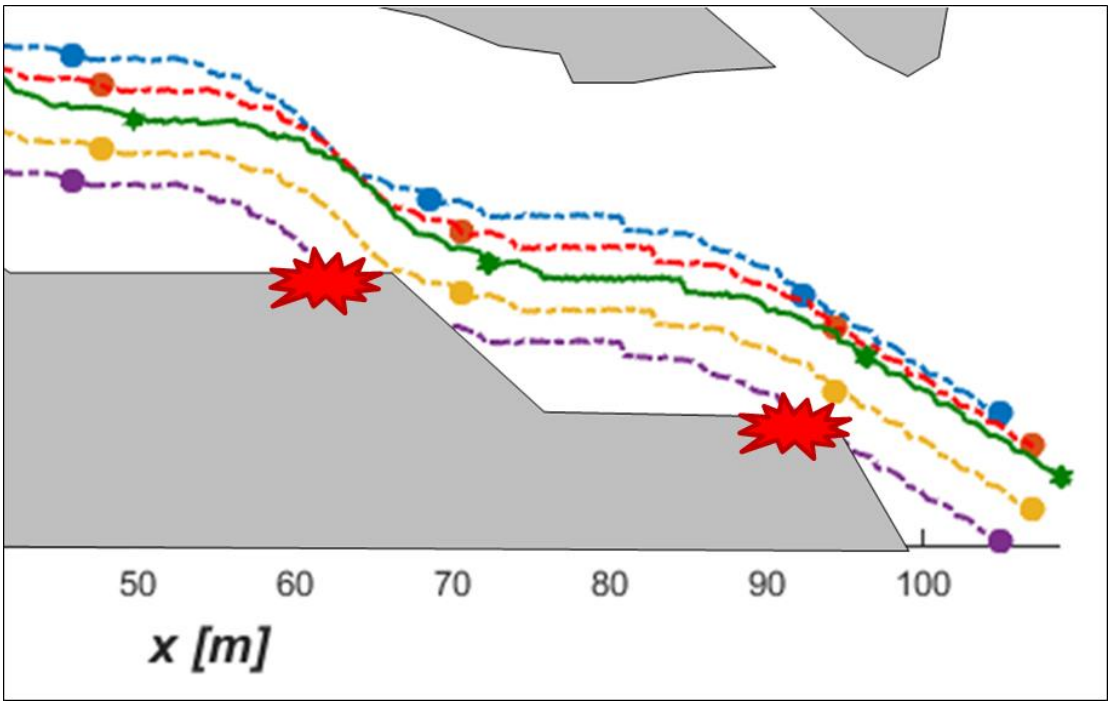

Figure 3.17 Enlarged Figure 3.16 in colliding situation

There are three reasons why a fleet of ships cannot avoid the collision situation. Firstly, a planned path is for a leader, hence static obstacles are not considered for the followers' paths. Secondly, equation (3.10) considered a position of the leader and relative deviations with the leader in the absence of obstacles, accordingly the algorithm did not consider the existence of the obstacles. Lastly, relative deviations δ_i in equation (3.10) are fixed values, for this reason it is impossible for a fleet to change a formation shape into a different formation.

To avoid the situation, the coordinated path planning strategy is proposed. The proposed strategy enables a fleet of ships to change a formation shape into a safer formation shape when a fleet face with static obstacles. The strategy applied the repulsive force vectors to equation (3.10) to change the formation shape. Therefore, the strategy enables the fleet not only to avoid the obstacles but also to maintain a formation.

In addition, a key idea of the strategy is that relative deviations δ_i of a formation vary in time in the presence of static obstacles. Applied repulsive force vectors adjust the deviations to avoid collision between the obstacles and a fleet of ships. To achieve the strategy, we define two types of formation shape. The first type called S_1 is a shape when a fleet of ships normally sail without static obstacles. The second type called S_2 considers a safer formation configuration than S_1 in that S_2 enable the fleet of ships to pass through confined channel or complex

waterway. Therefore, the fleet changes their formation shape from S_1 to S_2 , when the fleet approaches the static obstacles.

Here, there are four sections. Firstly, explanation of repulsive force vectors by potential field method is given. Secondly, the types of formation shapes, S_1 and S_2 are explained. Thirdly, the proposed coordinated path planning strategy is described. Lastly, simple examples of the strategy are given.

3.3.1. Repulsive force vector by potential field method

As shown in section 3.1.1, repulsive force vectors are calculated by the negative gradient of repulsive potential function.

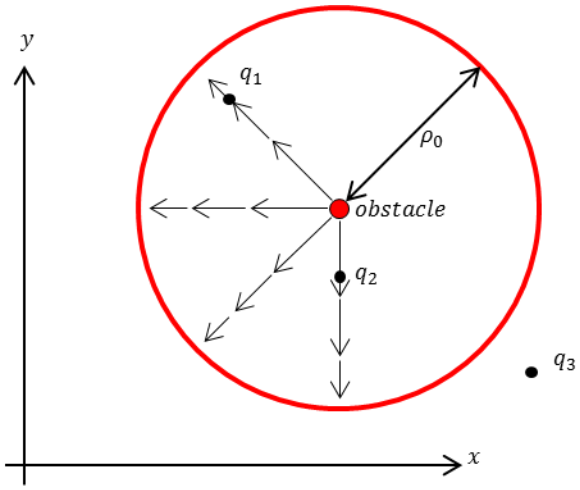

Figure 3.18 Repulsive force vector

Figure 3.18 shows the influence of obstacle ρ_0 and the repulsive force vector represented as single headed arrows from a point obstacle. There are three points where q_1 and q_2 are affected by the obstacle and q_3 is not influenced by the obstacle.

The repulsive force vectors at points q_1 and q_2 are given by $\vec{R}_{q1} = \left(\left|\vec{R}_{q1}\right|, \theta_{q1}\right)$ and $\vec{R}_{q2} = \left(\left|\vec{R}_{q2}\right|, \theta_{q2}\right)$. The magnitude and direction of $\vec{R}_{q1}$ and $\vec{R}_{q2}$ are represented by $\left|\vec{R}_{q1}\right|$, θ_{q1}, $\left|\vec{R}_{q2}\right|$ and θ_{q2}, respectively. Note that the point q_3 has no repulsive force vector because the distance between the obstacle and the point q_3 is longer than the influence of obstacle ρ_0. When we compare $\vec{R}_{q1}$ with $\vec{R}_{q2}$, the two repulsive force vectors differ from the magnitude and the orientation in that the points q_1 and q_2 are placed in different points.

3.3.2. Types of formation shapes

There are two types of formation shapes represented as S_1 and S_2. The reason why we need the different types of formation shapes is because a fleet of ships cannot go through narrow and confined obstacles if the size of the fleet cannot shrink into the smaller formation shape. This reason is clearly described in below figure.

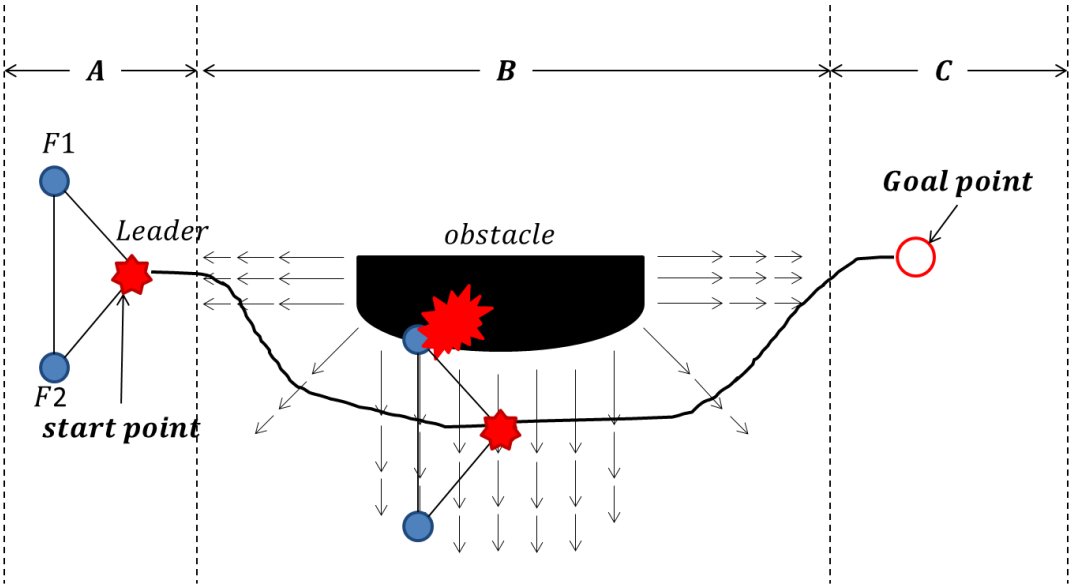

Figure 3.19 Path planning without the strategy on collision situation

As shown in Figure 3.19, there are one leader and two follower ships represented by star and circles. In addition, there are three intervals represented by A, B and C from start point to the goal point. Follower1 and follower2 are designated by F_1 and F_2. Figure 3.19 shows that a fleet of ships are supposed to go from start point in interval A to goal point in interval C. However, there is a collision of F_1 with the obstacle in interval B.

As mentioned above, there are two types of formation shapes, S_1 and S_2. Type of S_2 has a smaller width formation than type of S_1 to cross a narrow static obstacle. The type of S_2 is defined as a smaller width shape and a line shape in the following figure.

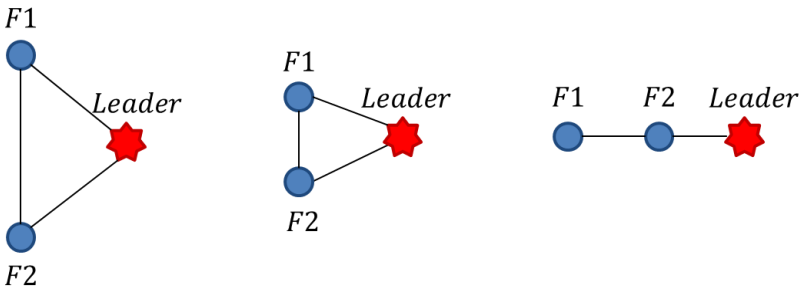

Figure 3.20 Types of formation shapes (left: S1, middle: S2.1 and right: S2.2)

As shown in Figure 3.20, there are three types of formation shapes in this study. Firstly, a formation shape on the left side is S_1 formed by triangular shape. Secondly, a smaller width

formation shape in the middle is $S_{2.1}$. Lastly, a line formation shape on the right-hand side is $S_{2.2}$.

3.3.3. Coordinated path planning strategy by repulsive force vector

To change the types of formation shapes from S_1 to S_2, proposed a coordinated path planning strategy uses repulsive force vectors. To understand clearly, in this chapter, a safer formation shape is designated as $S_{2.2}$ type. The strategy of changing S_1 type into S_2 type is described in Figure 3.21.

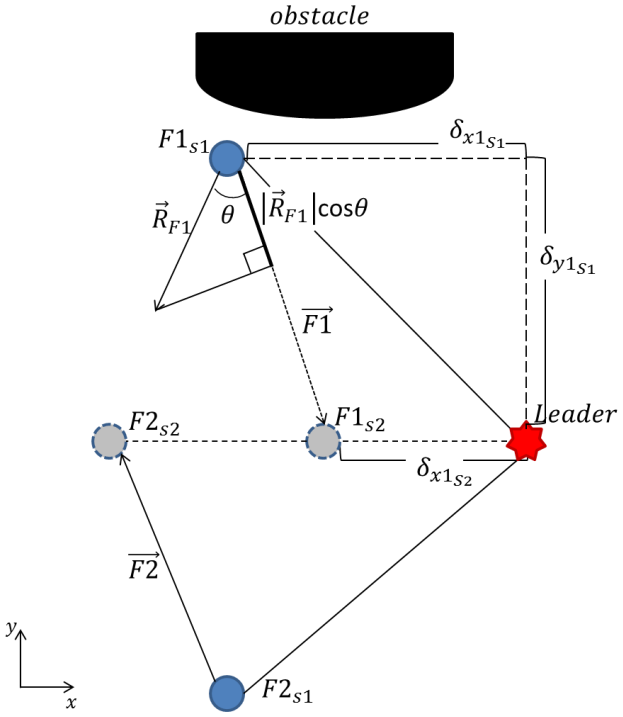

Figure 3.21 The strategy to change into safer formation shape

Figure 3.21 shows the process of shrinking triangular formation shape into a line formation in the presence of the static obstacle. A connection with each ship in S_1 type is represented as solid lines and a connection with each ship in S_2 type is represented as dotted lines. In addition, δ_{x1s1}, δ_{y1s1} and δ_{x1s2} are defined by the relative deviations of x and y directions of S_1 and S_2 types. $F1_{s1}$, $F2_{s1}$ are locations of follower1 and follower2 in S_1 type. $F1_{s2}$ and $F2_{s2}$ are locations of follower 1 and follower 2 in S_2 type. $\overrightarrow{F1}$ is the dotted arrow pointing from $F1_{s1}$ to $F1_{s2}$, which provide information of the desired direction to transform into S_2 type. $\vec{R}_{F1}$ is the repulsive force vector from the obstacle at the location of follower1, in addition, $|\vec{R}_{F1}|$ and θ are the magnitude of $\vec{R}_{F1}$ and the angle between $\vec{R}_{F1}$ and $\overrightarrow{F1}$, respectively. Furthermore, $|\vec{R}_{F1}|\cos\theta$ is scalar product of repulsive force vector $\vec{R}_{F1}$ and $\overrightarrow{F1}/|\overrightarrow{F1}|$, because $\vec{R}_{F1}$ and $\overrightarrow{F1}$,

θ can be calculated by $\theta = sign(\vec{R}_{F1} \times \overrightarrow{F1}) \cdot \cos^{-1}\left(\vec{R}_{F1} \cdot \overrightarrow{F1} / \left|\vec{R}_{F1}\right| \left|\overrightarrow{F1}\right|\right)$. Note that $sign(\cdot)$ is the function to return the sign of a real number $(\cdot)$. When the follower1 is affected by the repulsive force vector, the adjusted deviations of follower1 are illustrated in the following figure.

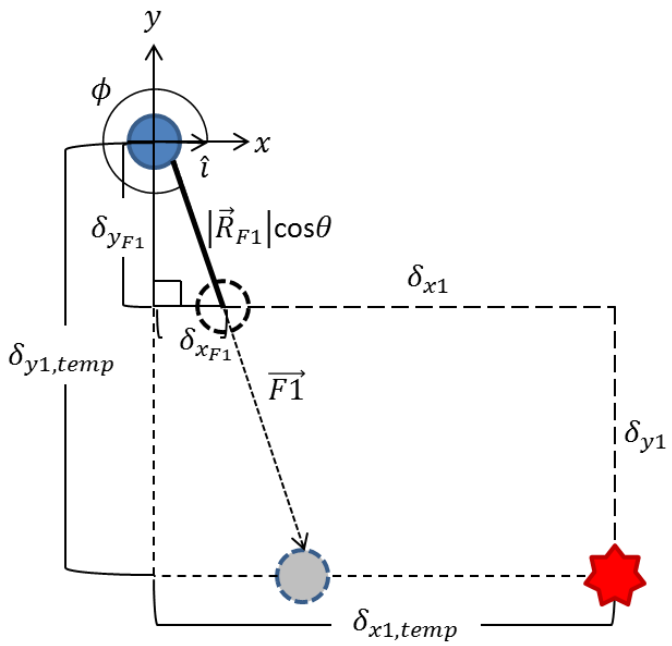

Figure 3.22 Adaptive deviation of follower1

As shown Figure 3.22, the adaptive deviations by x and y directions are denoted by $\delta_{x_{F1}}$ and $\delta_{y_{F1}}$, respectively. For the reason that $\overrightarrow{F1}$ and x direction unit vector $\hat{\imath}$ is known, the angle ϕ between $\overrightarrow{F1}$ and $\hat{\imath}$ can be obtained where it is calculated by $\phi = \text{sign}(\hat{\imath} \times \overrightarrow{F1}) \cdot \cos^{-1} \hat{\imath} \cdot \overrightarrow{F1} / \left|\overrightarrow{F1}\right|$. Therefore, the adaptive deviations are given by

$$\delta_{x_{F1}}(t) = k_x \cdot \left(\left|\vec{R}_{F1}\right| \cos\theta\right) \cos\phi \tag{3.12}$$

$$\delta_{y_{F1}}(t) = k_y \cdot \left(\left|\vec{R}_{F1}\right| \cos\theta\right) \sin\phi \tag{3.13}$$

k_x and k_y are gains of the adaptive deviations.

Finally, the relative deviations of followers are written by

$$\delta_{x1}(t) = \delta_{x1,temp}(t) - \delta_{x_{F1}}(t), \qquad \left(\delta_{x1s2} \le \delta_{x1} \le \delta_{x1s1}\right) \tag{3.14}$$

$$\delta_{y1}(t) = \delta_{y1,temp}(t) - \delta_{y_{F1}}(t), \qquad \left(\delta_{y1s2} \le \delta_{y1} \le \delta_{y1s1}\right) \tag{3.15}$$

In equations (3.14) and (3.15), δ_{x1} and δ_{y1} are the relative deviations of x and y direction with leader, respectively. In addition, $\delta_{x1,temp}$ and $\delta_{y1,temp}$ are temporary relative deviations. However, it is necessary to add saturation terms of the rate of δ_{x1} and δ_{y1} because high control input need to be avoided and smoother paths should be obtained

$$\dot{\delta}_{x1}(t) = \frac{\delta_{x1}(t+1) - \delta_{x1}(t)}{\Delta t} \qquad \left(\dot{\delta}_{x1,\min} < \dot{\delta}_{x1}(t) < \dot{\delta}_{x1,\max}\right) \tag{3.16}$$

$$\dot{\delta}_{y1}(t) = \frac{\delta_{y1}(t+1) - \delta_{y1}(t)}{\Delta t} \qquad \left(\dot{\delta}_{y1,\min} < \dot{\delta}_{y1}(t) < \dot{\delta}_{y1,\max}\right) \tag{3.17}$$

In equations (3.16) and (3.17),(3.16) (3.16) $\dot{\delta}_{x1}(t)$ and $\dot{\delta}_{y1}(t)$ are the rate of δ_{x1} and δ_{y1} , which are boundary between minimum rate and maximum rate. When the equations (3.14) (3.15), (3.16) and (3.17) are applied to the equation (3.10) in the case of collision situation in Figure 3.19, The behaviour of the fleet is described in the following figure.

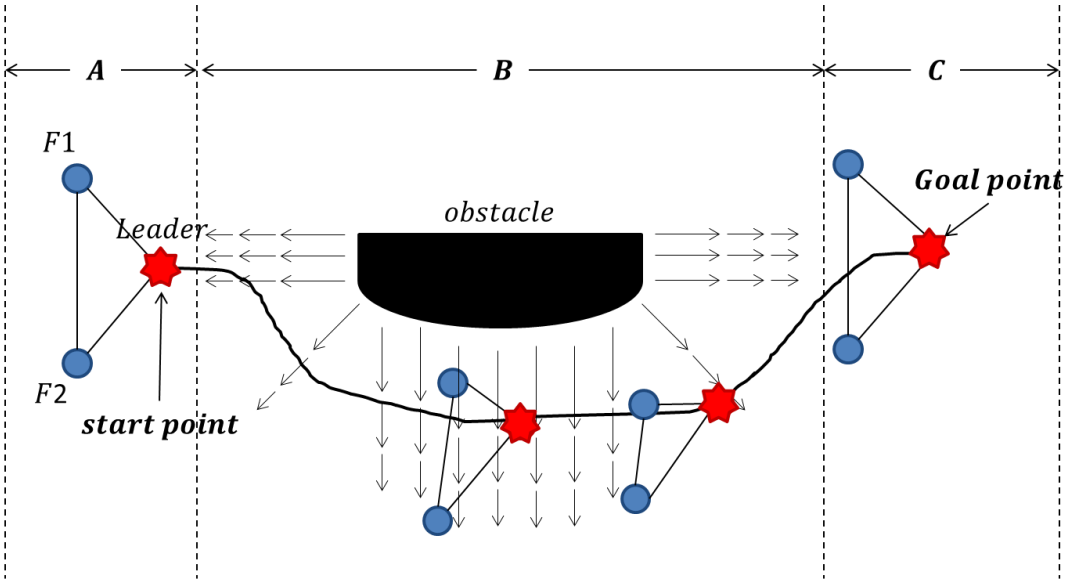

Figure 3.23 Path planning with the strategy on collision situation

Figure 3.23 shows that a fleet of three ships reach the goal point and avoid collision situation with the obstacle by changing the types of formation shapes. Because $F1$ can change into a line formation shape from triangular formation shape by using the proposed strategy, $F1$ formed a horizontal line with a leader as approaching the obstacle. After crossing the obstacle,

$F1$ reshaped to triangular formation shape in interval C. On the other hand, while the leader was in the process of moving from the start point to the goal point, $F2$ did not change the formation shape for the reason that $F2$ was not affected by repulsive force vector from the obstacle.

3.4. Examples

In this chapter, to verify the strategy of planning coordinated paths for a fleet of ships, simulation examples were performed for one leader ship and two follower ships in the presence of simple obstacles. It shows that a fleet of ships avoid the obstacles by changing the formation shapes while going into a goal point from a start point. In addition, this section discusses about the relative deviations of follower1 and follower2 with the leader while avoiding the obstacles.

Three different cases of simulations are operated. Firstly, a static obstacle is located at the bottom of the map. Secondly, the obstacle is located at the top of the map. Lastly, two static obstacles are located at the bottom and the top of the map. In all cases, a start point and a goal point are given by $(50,125)$ and $(960,150)$. In addition, S_1 type is a triangular formation and S_2 type is designated a line formation. Specific configurations of S_1 type of follower1 and follower2 are designated by $(\delta_{s1x1},\delta_{s1y1})=(-50,30)$ and $(\delta_{s1x2},\delta_{s1y2})=(-50,-30)$. Configurations of S_2 type of follower1 and follower2 are designated by $(\delta_{s2x1},\delta_{s2y1})=(-35,0)$ and $(\delta_{s2x2},\delta_{s2y2})=(-70,0)$. Moreover, there are eleven triangle connections which describe the moving process for a fleet of ships to reach the goal point from the start point.

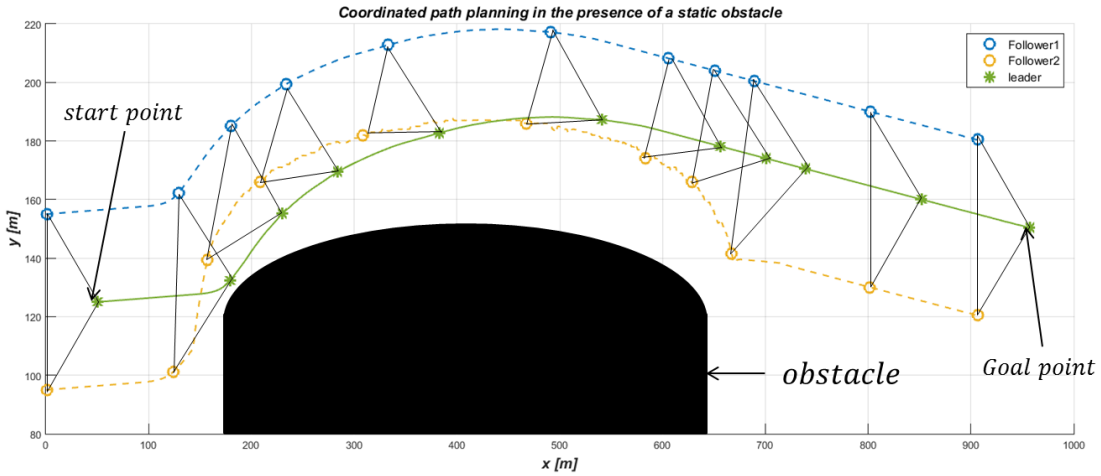

Figure 3.24 Coordinated path planning in case1

A path of the leader was described by a solid line and paths of two followers were described by dotted lines. The triangular formation defined by S_1 type for a fleet of ships was formed at the start point. However, the triangular formation was transformed slightly as the fleet of ships approach the obstacle in that follower2 was changing into a horizontal line formation. In the fifth triangle connection, follower2 was totally set as a line formation called S_2 type. After the

fifth triangle connection, follower2 reshaped to S_1 type from S_2 type because follower2 was less affected by the repulsive force vectors from the obstacle. In the tenth triangle connection, S_1 type was formed again since there is no influence of the obstacle.

The relative deviations of follower1 and follower2 are described in following figure.

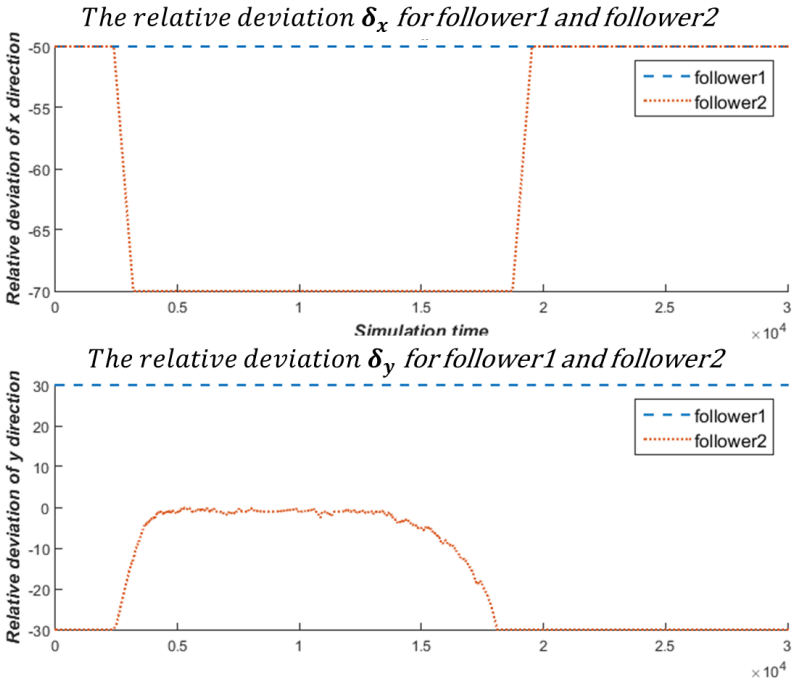

Figure 3.25 Relative deviation of follower1 and follower2 in case1

As shown in Figure 3.24 and Figure 3.25, the relative deviations of follower1 were not changed because follower1 was not influenced by the obstacle. However, the relative deviations of follower2 were adjusted while follower2 avoided the obstacle. The relative deviations of follower2 $(\delta_{x2}, \delta_{y2})$ approximately converged to $(-70, 0)$ in the presence of the obstacle. After avoiding the obstacle, $(\delta_{x2}, \delta_{y2})$ went gradually back to $(-50, -30)$.

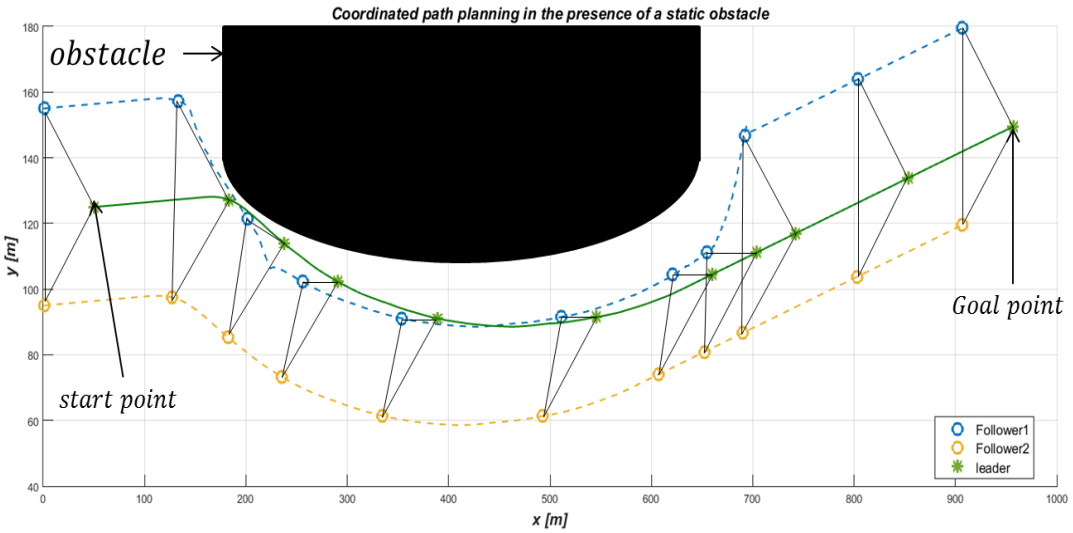

Figure 3.26 Coordinated path planning in case2

In Figure 3.26, the same obstacle is situated at the top of the map in case2. In that case, repulsive force vectors by the obstacle have an influence on follower1. The first and the second triangle connections were not transformed, on the other hand, the fleet of ships were reshaping the formation from the third triangle connection to eighth triangle connection because follower1 approached closely the obstacle. During the process of reshaping, the formation shape of follower1 was transformed into a line formation. After the process, the fleet of ships returned to the original formation shape, similarly with the case1.

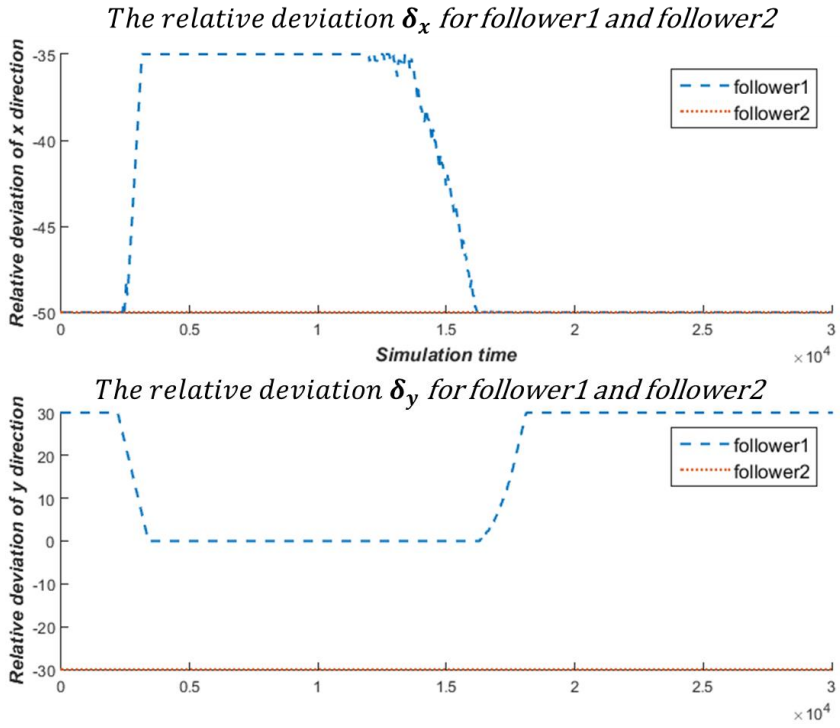

Figure 3.27 Relative deviation of follower1 and follower2 in case2

Figure 3.27 shows the relative deviations on x and y axis during a simulation of the case2. The relative deviations of follower2 had a constant value during the simulation of case2, because the distance of the obstacle's influence did not reach to follower2. On the contrary, the relative deviation of follower1 on x axis, δ_{x1} went up to -35 and the relative deviation of follower1 on y axis, δ_{y1} went down to 0 when follower1 faced with the obstacle. The relative deviations of follower1 maintained fixed values while follower1 passed through the obstacle because the relative deviations are bounded. After a fleet of ships went through the obstacle, the relative deviations of follower1 returned to form the original formation shape.

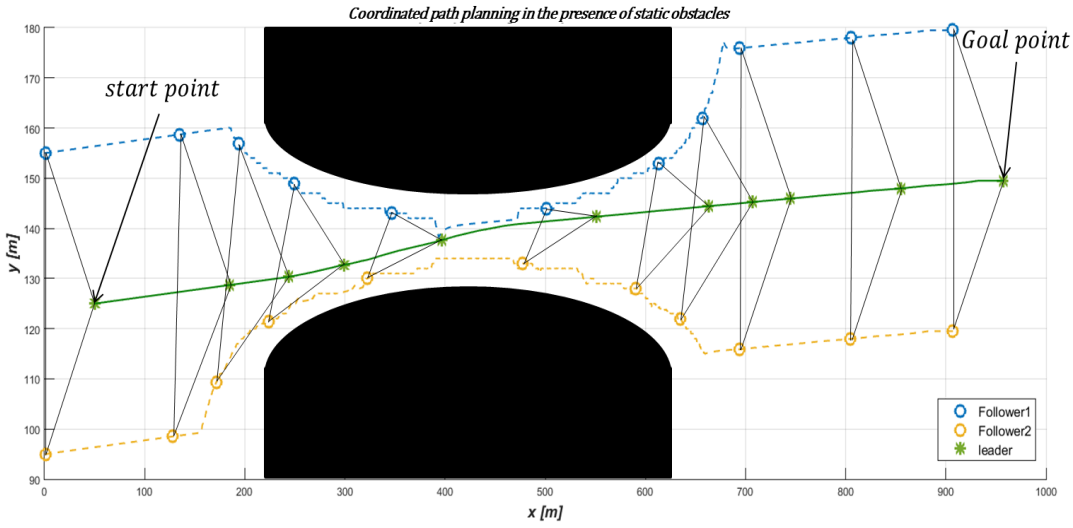

Figure 3.28 Coordinated path planning in case3

Two obstacles that are in the top and the bottom of the map are used in case3. Because the width between two obstacles is narrow, it is a more complicated simulation case for the fleet of ships to avoid narrow obstacles.

As a result, the fleet of ships avoided the obstacles without collision while moving to the goal point. There are three steps to pass through the obstacles. Firstly, the type of formation shape was S_1 at the first triangle connection and the second triangle connection. Secondly, the size of connection triangles was shrunk from the third connection triangle to the sixth connection triangle, because both of followers were affected by the repulsive force vectors of the obstacles. It is the process of changing S_1 type into S_2 type. Lastly, after the sixth connection triangle, the size of connection triangle was expanded, and the fleet of ships reshaped S_1 type.

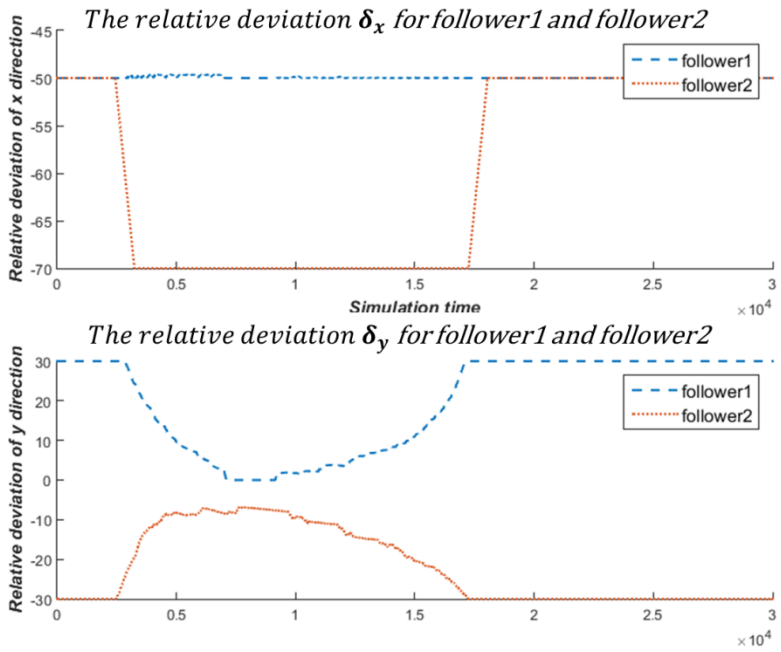

Figure 3.29 Relative deviation of follower1 and follower2 in case3

As shown in Figure 3.28, there are the two obstacles that give an influence on both followers. Therefore, there was a tendency to shrink the size of the formation shape when the fleet approached the obstacles and there was a tendency to expand the size of the formation shape after the fleet passed the obstacles through. However, in Figure 3.29, the relative deviation δ_{x1} was not changed into -35 that is the value of δ_{s2x1} even though follower1 came near the obstacle at the top. Because follower1 was only affected by vertical repulsive force vectors from the obstacle, the relative deviation on y axis, δ_{y1} was only adjusted.

In conclusion, three cases of examples about coordinated path planning in the presence of obstacles are considered. The results show the proposed coordinated path planning strategy enable the fleet deal with three different obstacle configurations in the map. As a result, the followers can adjust relative deviations with a leader and the fleet can change their formation shapes into a safer formation in dangerous situations. Therefore, coordinated paths for followers were generated without collisions with not only obstacles but also each ship.

Chapter 4. Simulation

To validate the proposed strategy, simulations have been carried out for five unmanned surface ships model being defined as a point mass model with full actuation in two cases with different formation types, which are a smaller width formation shape named $S_{2.1}$ and a line formation shape named $S_{2.2}$. These simulations assumed that the leader of the fleet can obtain the information of the planned path and the four followers can obtain the position information of each ship. In addition, the repulsive force vectors by the static obstacles are provided to the followers. It is also assumed that the fleet of five unmanned surface ships manoeuvres without environmental disturbances such as wind, waves, ocean currents forces and moments.

This chapter is divided into three sections. Section 4.1 introduces map representation, initial setup of formation types and initial positions of the fleet. Section 4.2 shows trajectories for the fleet and relative deviations with the leader. Lastly, the simulation results are discussed.

4.1. Basic configuration of simulations

4.1.1. Map representation

This section considers more complex static obstacles which form a bottle-neck. The size of the map in these simulations is $1200[m]\times 450[m]$. A start point and a goal point in the map are described in Figure 4.1.

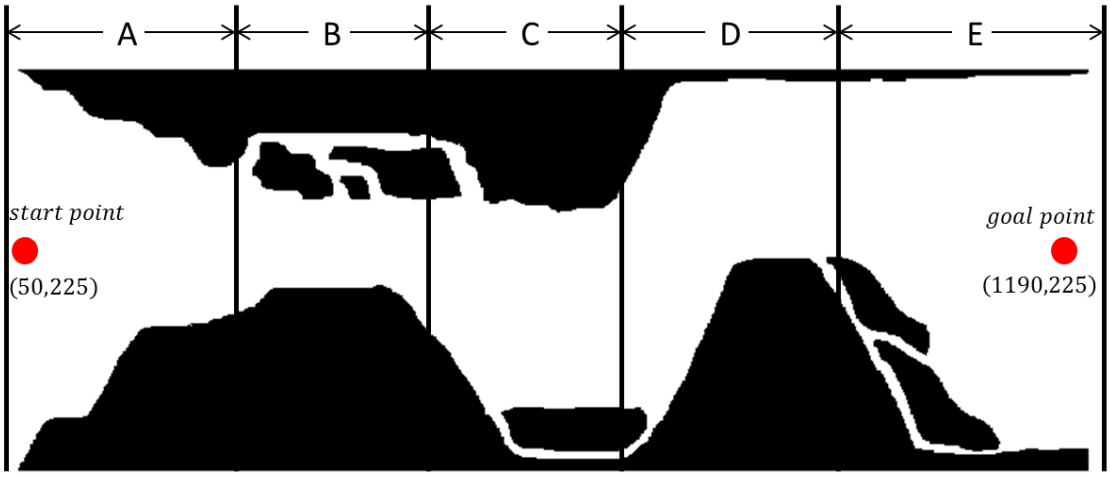

Figure 4.1 Map configuration with start point and goal point

To show a detail process of changing formation for the fleet in the simulations, the map is divided into five parts. Part A represents gradually decreasing width of channel. Part B shows constant width of channel. Part C illustrates gradually increasing width of channel on the underside. On the other hand, part D describes increasing width of channel on the topside. Finally, part E shows increasing width of channel on the both sides. In terms of the five parts in the map, the fleet of the unmanned surface ships changes their formation while passing through the static obstacles by using the proposed strategy.

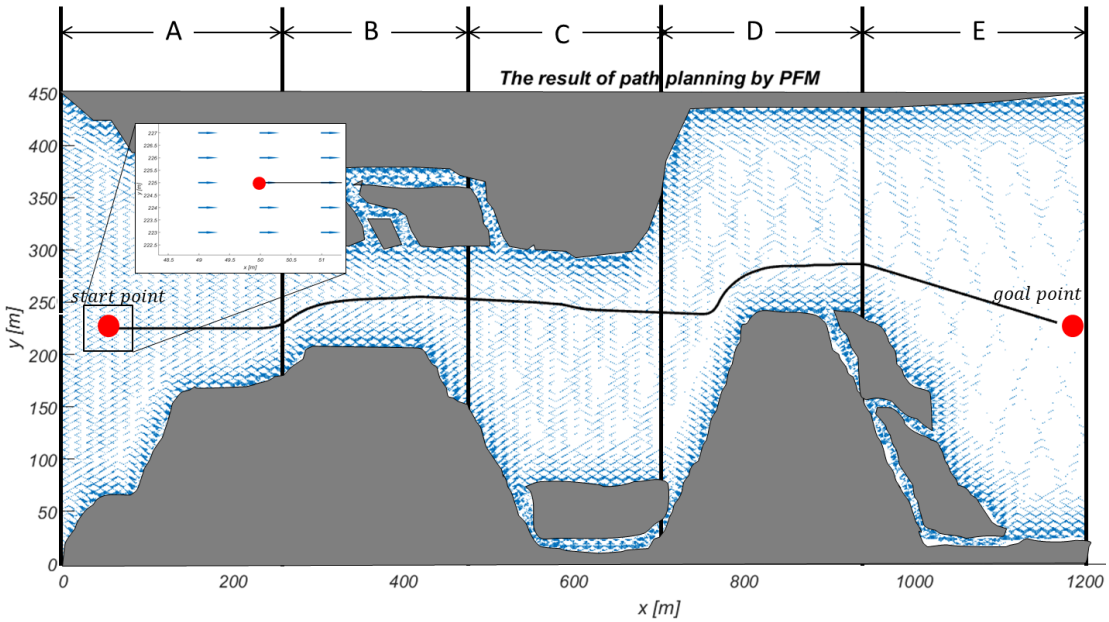

Figure 4.2 A planned path by PFM

Figure 4.2 shows the path for the leader from the start point to the goal point in the presence of the static obstacles and the force vectors represented as blue arrows. The path for the leader can avoid the static obstacles and reach the goal point by using PFM.

4.1.2. Initial setup for simulations

To generate a coordinated path planning for the fleet, configuration of desired formation types and communication topology for formation control should be considered. This section shows the configuration, an adjacent matrix related to the communication topology and initial positions for the fleet.

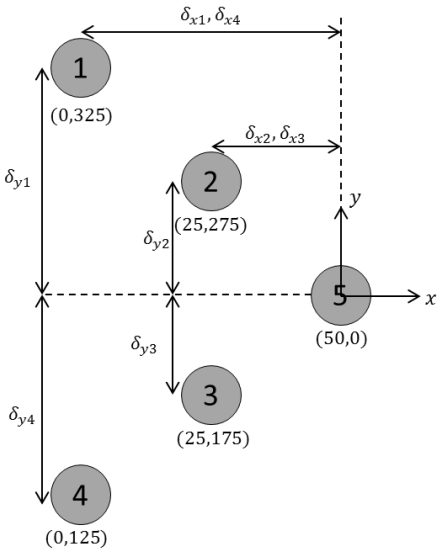

Figure 4.3 Configuration of formation shape

Figure 4.3 shows the configuration of formation shape and the initial positions for the fleet in the simulations. The numbers in circles represent follower1, follower2, follower3, follower4 and leader designated as number 5. In addition, $\delta_{xn}, \delta_{yn} (n = 1, \ldots, 4)$ mean horizontal and vertical distances relative with the leader defined as the origin of the coordinate. Therefore, the formation configuration of types, S_1, $S_{2,1}$ and $S_{2,2}$ is written in Table 1.

	S_1	$S_{2,1}$	$S_{2,2}$
$(\delta_{x1}, \delta_{y1})$	$(-50, 100)$	$(-50, 50)$	$(-50, 0)$
$(\delta_{x2}, \delta_{y2})$	$(-25, 50)$	$(-25, 25)$	$(-25, 0)$
$(\delta_{x3}, \delta_{y3})$	$(-25, -50)$	$(-25, -25)$	$(-12.5, 0)$
$(\delta_{x4}, \delta_{y4})$	$(-50, -100)$	$(-50, -50)$	$(-37.5, 0)$

Table 1 Formation configuration of three different types

In addition, the adjacent matrix related to communication topology is described in Figure 4.4.

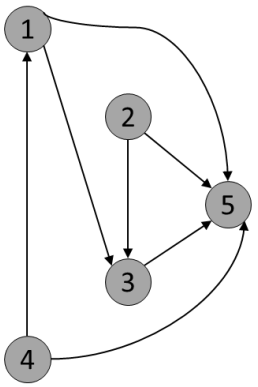

$$A = \begin{bmatrix} 0 & 0 & 1 & 0 & 1 \\ 0 & 0 & 1 & 0 & 1 \\ 0 & 1 & 0 & 0 & 1 \\ 1 & 0 & 0 & 0 & 1 \\ 0 & 0 & 0 & 0 & 0 \end{bmatrix}$$

Figure 4.4 Adjacent matrix related to communication topology

4.2. Simulation results

This section presents the simulation results for the proposed strategy with two different safer formation types to investigate the feasibility of the strategy. Additionally, simulation results describe the trajectories of the fleet which generates coordinated paths and illustrate results of time-varying relative deviations with the leader to show detail explanations of changing formations.

4.2.1. Case1: Simulation result

In this first simulation case, the fleet of five unmanned surface ships is required to move to the goal point with formation shape of S_1 type and $S_{2,2}$ type in the presence of static obstacles. As mentioned in section 4.1.1, the map is divided into 5 intervals to describe shrinking behaviours and expanding behaviours of the fleet, respectively. With the initial setup in section 4.1.2, the entire trajectories of the fleet is shown in Figure 4.5.

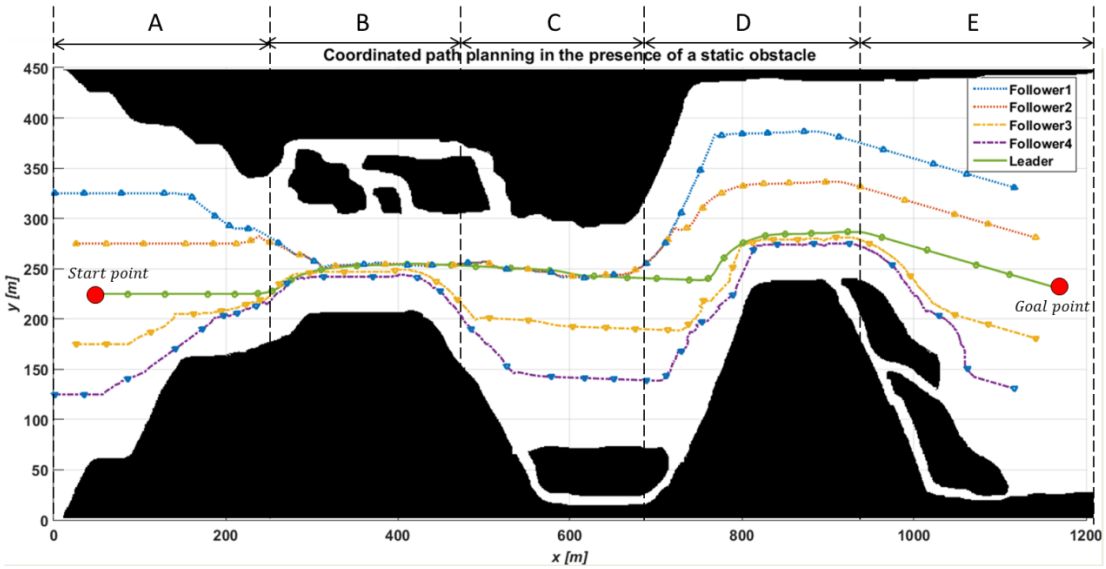

Figure 4.5 Coordinated paths for the fleet in the simulation of case1

Figure 4.5 shows the coordinated paths for the fleet where blue upward-pointing triangles and yellow upward-pointing triangles is represented as follower1-2 (equally means that "from follower1 to follower2") and yellow downward-pointing triangles and blue downward-pointing triangles is designated as follower3-4, in addition, green circle is represented as leader. It showed that the fleet can avoid the static obstacles by changing pre-defined formation shape, S_1 into a safer formation shape, $S_{2,2}$ while passing through the static obstacles. As we expected in section 4.1, the fleet of the five ships shrunk the size of formation type S_1 in the end of part A in order to transform into $S_{2,2}$ type. In part B, follower1-2 and leader was successfully changed into the line formation shape. However, follower3-4 and leader were not totally shrunk into the line formation type. Because of changing pattern of the static obstacles in part C, follower3-4 were expanded into the original formation shape, S_1. On the other hand, follower1-2 and leader maintained the line formation shape because of upper static obstacles. In part D, follower1-2 were expanded as the width between leader and the obstacles on upper side in the map was increased. In addition, follower3-4 and leader were transformed into the line formation shape to avoid the obstacles. Lastly, follower3-4 were reshaped into the triangular formation shape. The fleet of five ships could reach the goal point with the original formation shape.

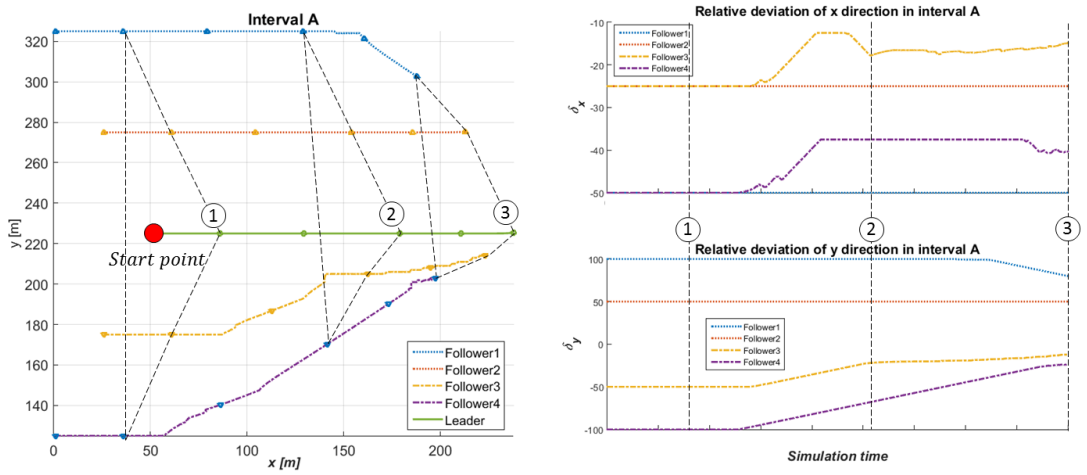

Figure 4.6 Coordinated paths and relative deviations in interval A

Figure 4.6 shows the coordinated paths for the fleet on the left-hand side figure and the relative deviations on the right-hand side figure while the fleet passed through interval A. To represent the current state of the formation for the fleet, in these simulations, three dotted connection lines and three numbers are used in the map. For example, on the left figure, there are three dotted connection lines designated as ①, ②, and ③. At the first dotted connection line ①, because there are no influences of the obstacles, the shape of formation and the relative deviations for the fleet were constantly maintained. However, because follower3-4 were affected by the underside obstacles at the second dotted connection line ②, the formation shape of follower3-4 was changing into the safer type of formation, $S_{2,2}$. Additionally, the relative deviations of x direction for follower1-2 were increased to shrink the size of the formation shape. The third dotted connection line ③ shows that not only follower3-4 but also follower1-2 were changing into the safer formation shape because of influence by the obstacles on both sides.

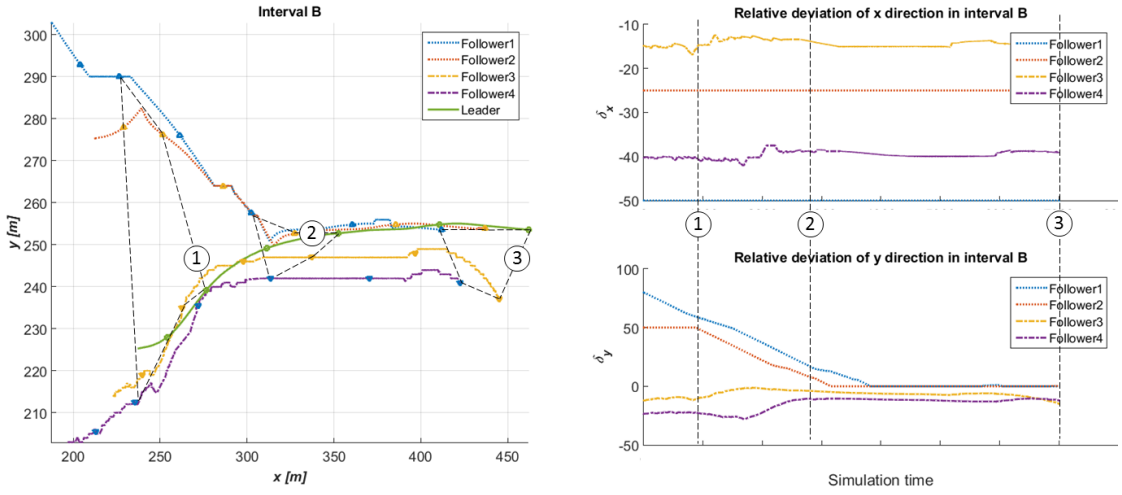

Figure 4.7 Coordinated paths and relative deviations in interval B

In Figure 4.7, the width between the obstacles on both sides is gradually decreased in the map. Therefore, the size of the formation shape should be shrunk in the process of going through interval B to avoid a bottle-neck pattern of the obstacles. At the first dotted connection line ①, δ_y of follower1-4 were gradually converged into zero in order to change S_1 type into $S_{2,2}$ type. On the other hand, δ_x of follower1-4 were not changed significantly because the fleet was less influenced by horizontal repulsive force vectors than by vertical repulsive force vectors. Follower1-2 and leader were successfully transformed into the line formation shape, on the other hand, follower3-4 were expanded between the second dotted connection line ② and the third dotted connection line ③.

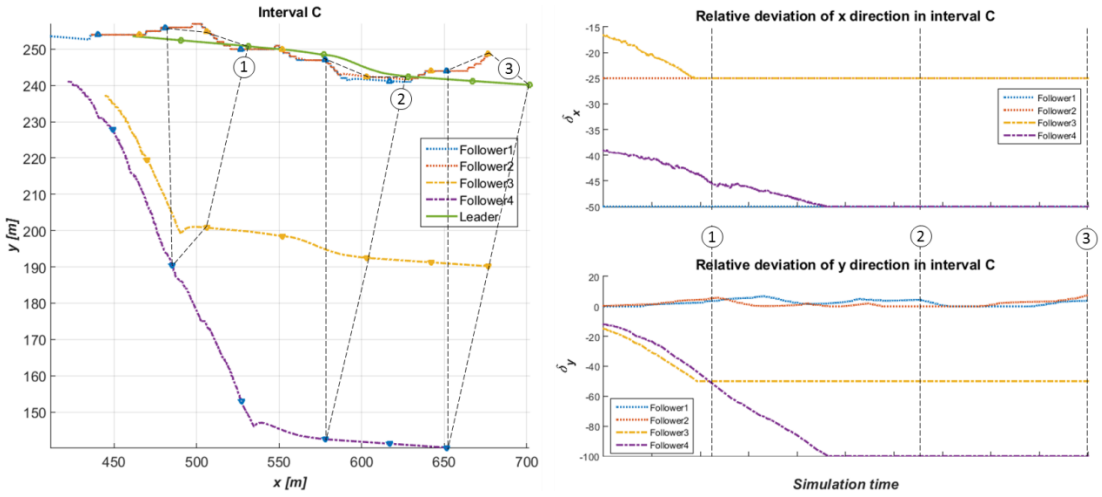

Figure 4.8 Coordinated paths and relative deviations in interval C

Figure 4.8 shows the process of totally expanding the size of formation shape of follower3-4 and maintaining the formation type, $S_{2,2}$ for follower1-2 and leader. As there is no influence of the obstacles on bottom side, follower3-4 can be changed into the original formation shape, S_1 in interval C. However, the formation of follower1-2 was maintained to overcome the obstacles on topside. In a similar aspect, δ_y of follower1-2 was slightly oscillated around zero in interval C because the pattern of the obstacles on topside does not have flat surfaces.

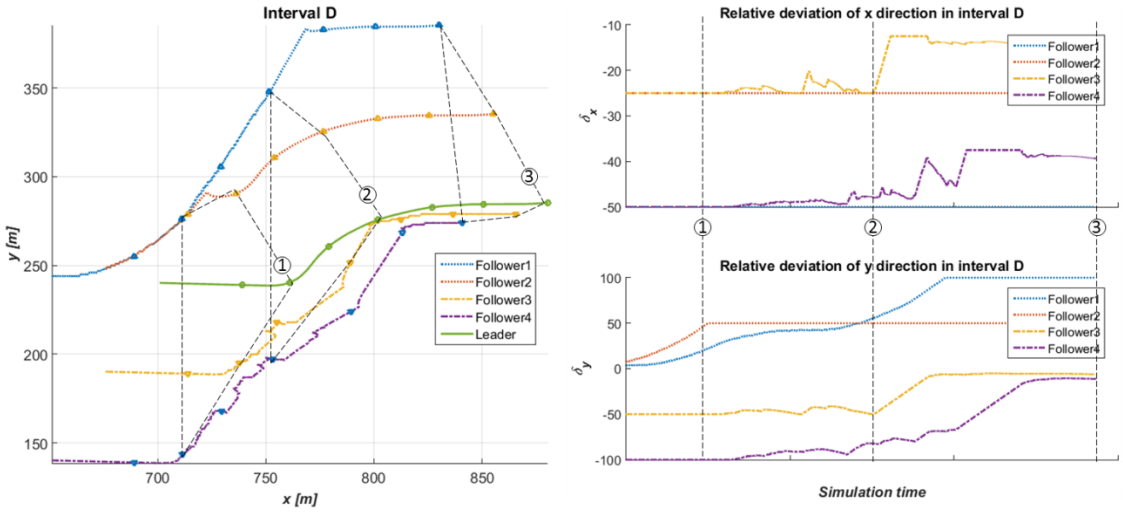

Figure 4.9 Coordinated paths and relative deviations in interval D

Similarly, Figure 4.9 shows that the formation of follower1-2 was expanded into S_1 type and the formation of follower3-4 was shrunk in order to avoid the obstacles at the same time. At the second dotted connection line ②, follower1-2 were in the process of changing a formation type into S_1 type, however, the formation of follower3-4 was changed into $S_{2,2}$ type. At the third dotted connection line ③, the formation of follower1-2 was successfully transformed into the triangular type and follower3-4 were almost changed into the line formation shape.

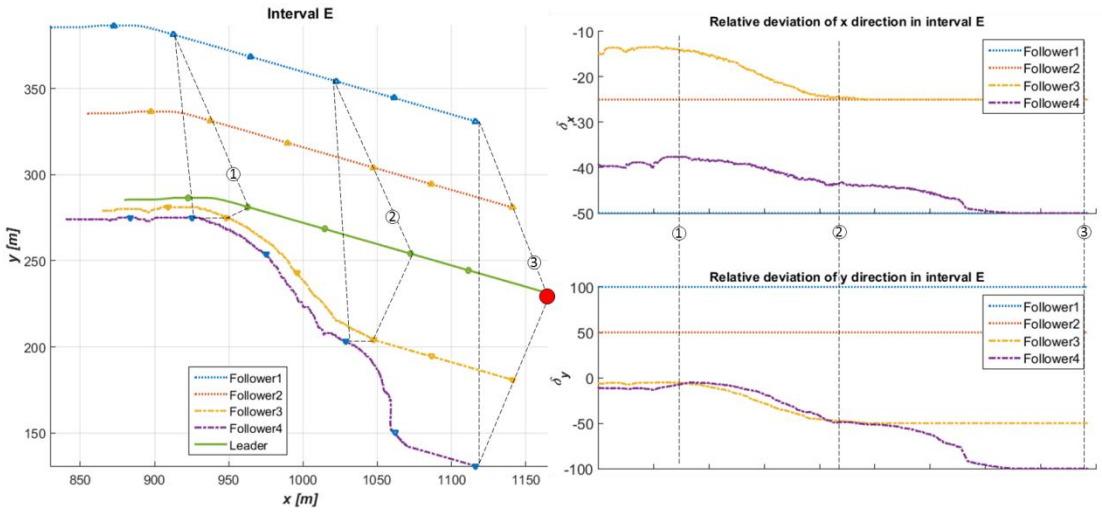

Figure 4.10 Coordinated paths and relative deviations in interval E

Figure 4.10 shows that the fleet reaches the goal point with the original formation. In interval E, δ_x and δ_y of follower1-2 were steady because there are no repulsive force vectors by the obstacle on top side. At the first dotted connection line ①, follower3-4 were significantly influenced by the obstacles on bottom side. However, δ_x and δ_y of follower3-4 were going down until the second dotted connection line ②. In addition, δ_x and δ_y of follower3 were

converged toward constant values, where it means that follower3 was completely changed into the formation type, $S_{2,2}$. Finally, δ_x and δ_y of follower1-4 were converged toward constant values and the formation of the fleet were completely reshaped into the original triangular formation type at the third dotted connection line ③.

4.2.2. Case2: Simulation result

In case2, the formation S_2 type for the fleet is different from the formation type of case1 in that the formation type $S_{2,1}$ is triangular and the width of the type is wider than $S_{2,2}$ type. this case was simulated to investigate the feasibility of the proposed strategy applying on various formation shapes.

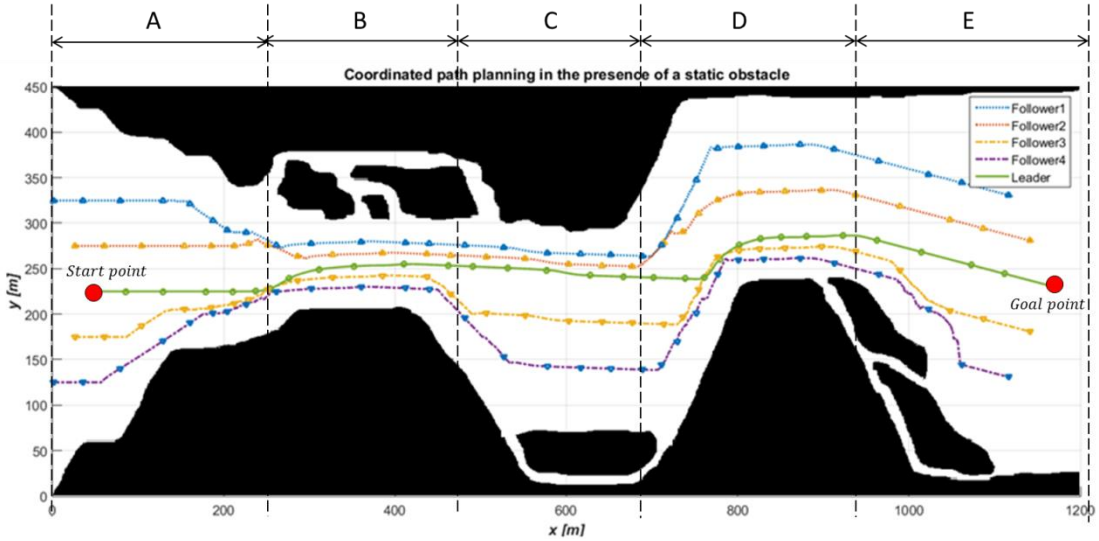

Figure 4.11 Coordinated paths for the fleet in the simulation of case2

Figure 4.11 shows that the fleet of five unmanned surface ships can change their formation shape into the safer formation type to avoid a bottle-neck obstacle in the process of moving to the goal point from the start point. Similarly with Figure 4.5 in case1, the size of the fleet was shrunk to change their formation into $S_{2,1}$ type in interval A. During interval B, the fleet was completely changed into $S_{2,1}$ type while going through the obstacles. In the next interval C, follower3-4 were expanded into S_1 type, on the other hand, the formation type of follower1-2 was maintained as $S_{2,1}$ shape. Contrary to interval C, the formation of follower1-2 was changed into S_1 type, in addition, follower3-4 moved to form $S_{2,1}$ type. In interval E, the fleet of the five ships was totally expanded into the original formation shape again when leader safely reached the goal point.

In addition, detail descriptions of the behaviours for the fleet in interval A-E are can be found in Appendix D with brief explanations.

Chapter 5. Discussion, Conclusion and Further Work

After this thesis reviewed previous published paper in Chapter 2, it is decided to research coordinated path planning strategy dealing with formation reconfiguration and formation changing to avoid static obstacles. Hence the overall aim of this research was to contribute to the realisation of unmanned navigation for a fleet of unmanned surface ships. To achieve the aim, the methodology for coordinated path planning strategy was proposed and it was verified by performing simulations.

The proposed methodology is divided into three parts in order to solve three problems that are path planning for a leader, maintaining a formation while tracking a path and avoiding obstacles while maintaining the formation. Three solutions to the problems are 'Potential field method', 'Consensus algorithm', and 'proposed coordinated path planning strategy'. A lot of research on 'Potential field method' and 'Consensus algorithm' have already been studied and have been used for commercial purposes because they can be simply applied and easily understandable. Therefore, two solutions were combined with the advantages to propose coordinated path planning in the presence of static obstacles. Finally, the proposed strategy used repulsive force vectors by obstacles to change their formation into a safer formation.

To verify the proposed methodology, two cases of simulations have been carried out. The assumptions of these simulations are that leader knows information of the path, repulsive force vectors are given to followers, there are no environmental disturbances, and unmanned surface ship models are defined as point mass models. The simulation results show that the proposed strategy enables a fleet of multi unmanned surface ships to avoid bottle-neck shaped static obstacles and to reach a goal point from a start point.

These simulations were put effort into dealing with five problems from literature review, Chapter Chapter 2. Firstly, a few published results did not show that a group of vehicles is changed into an original formation shape after avoiding static obstacles(Arrichiello, Chiaverini et al. 2006), (Desai, Ostrowski et al. 1998), and (Liu, Bucknall 2015). These simulation results show not only the process of changing formation types while passing through static obstacles but also the process of being reshaped into an original formation type after passing the static obstacles. Secondly, even though Chen, (2008) showed the whole process of switching formation types in the presence of static obstacles, we cannot realize collision situations with each vehicle for the reason that there are no detail descriptions during the process of changing formation types. In these simulations, the map is divided into five intervals to describe whether a fleet collide with each ship in detail. Figure 4.6 to Figure 4.10 show the result of trajectories for a fleet, where it showed whether the fleet collides with each ship or not. Thirdly, even if Fan, (2010) proposed collision free formation changing control algorithm, the algorithm works when only two or more AUVs perceive dangerous situations. Compared with Fan, (2010), the proposed strategy uses repulsive force vectors which influence all follower of the fleet to avoid the obstacles. Therefore, the formation of the fleet can be individually changed into other formation type by using the proposed strategy even though only one follower is affected by the obstacles. Additionally, Radovnikovich, (2014) has a drawback of efficiency in that both wings of formation should be switched into a line formation shape even if a group of vehicles

approaches one sided obstacle. The proposed strategy enables the fleet to avoid one sided static obstacles efficiently in Figure 4.8 and Figure 4.9. One wing of formation can be changed into a line formation shape when the fleet passes through one sided static obstacles because of repulsive force vectors by the obstacles, however, the other wing of the formation is maintained. Finally, inherent shortcoming of switching formation strategy is dealt with, which is sudden change of position errors for followers now that a group of robots decides to switch formation pattern to avoid static obstacles. The proposed strategy can adjust relative deviations to change their formation type when the fleet is affected by static obstacles. Therefore, it can prevent sudden changes of position errors while the fleet changes formation in Figure 4.6 to Figure 4.10.

Finally, the main conclusions drawn from the research presented in the thesis can be summarized as follows:

- ✓ A critical review of the state-of-the-art algorithms for path planning, formation control and coordinated path planning disclosed important problems were not addressed in previous works

- ✓ 'Potential field method' and 'Consensus algorithm' are used to devise a strategy of coordinated path planning based on three behavioural assumptions. A coordinated path planning strategy for multi unmanned ships to avoid static obstacles was presented in this study. This strategy is suitable for changing formation shapes to pass through the static obstacles without collisions.

- ✓ Simulation environment of the devised strategy was developed in MATLAB/Simulink. Feasibility and efficiency of the devised strategy was investigated in the simulation environment. The strategy has been proven a useful method for coordinated path planning.

While this study has demonstrated the potential of coordinated path planning for a fleet of unmanned surface ships in the presence of static obstacles, many opportunities for extending the scope of this study remain. For future work, the proposed methodology will be extended to deal with kinetic models for unmanned ships. In addition, future work includes taking into account environmental disturbances such as wind, waves and ocean currents.

REFERENCES

ARRICHIELLO, F., CHIAVERINI, S. and FOSSEN, T.I., 2006. Formation control of marine surface vessels using the null-space-based behavioral control. *Group Coordination and Cooperative Control.* Springer, pp. 1-19.

ASL, A.N., MENHAJ, M.B. and SAJEDIN, A., 2014. Control of leader–follower formation and path planning of mobile robots using Asexual Reproduction Optimization (ARO). *Applied Soft Computing,* **14**, pp. 563-576.

BAJODAH, A.H., HODGES, D.H. and CHEN, Y., 2003. New form of Kane's equations of motion for constrained systems. *Journal of Guidance, Control, and Dynamics,* **26**(1), pp. 79-88.

BALCH, T. and ARKIN, R.C., 1998. Behavior-based formation control for multirobot teams. *IEEE Transactions on Robotics and Automation,* **14**(6), pp. 926-939.

CAMPBELL, S., NAEEM, W. and IRWIN, G.W., 2012. A review on improving the autonomy of unmanned surface vehicles through intelligent collision avoidance manoeuvres. *Annual Reviews in Control,* **36**(2), pp. 267-283.

CAO, Y.U., FUKUNAGA, A.S. and KAHNG, A., 1997. Cooperative mobile robotics: Antecedents and directions. *Autonomous robots,* **4**(1), pp. 7-27.

CEN, Y., WANG, L. and ZHANG, H., 2007. Real-time obstacle avoidance strategy for mobile robot based on improved coordinating potential field with genetic algorithm, *Control Applications, 2007. CCA 2007. IEEE International Conference on* 2007, IEEE, pp. 415-419.

CHEN, X. and LI, Y., 2008. Stability on adaptive NN formation control with variant formation patterns and interaction topologies. *International Journal of Advanced Robotic Systems,* **5**(1), pp. 8.

CHEN, Y.Q. and WANG, Z., 2005. Formation control: a review and a new consideration, *Intelligent Robots and Systems, 2005.(IROS 2005). 2005 IEEE/RSJ International Conference on* 2005, IEEE, pp. 3181-3186.

CHOSET, H.M., 2005. *Principles of robot motion: theory, algorithms, and implementation.* MIT press.

DAI, Y., KIM, Y., WEE, S., LEE, D. and LEE, S., 2015. A switching formation strategy for obstacle avoidance of a multi-robot system based on robot priority model. *ISA transactions,* **56**, pp. 123-134.

DESAI, J.P., OSTROWSKI, J. and KUMAR, V., 1998. Controlling formations of multiple mobile robots, *Robotics and Automation, 1998. Proceedings. 1998 IEEE International Conference on* 1998, IEEE, pp. 2864-2869.

FAN, S., FENG, Z. and LIAN, L., 2010. Collision free formation control for multiple autonomous underwater vehicles, *OCEANS 2010 IEEE-Sydney* 2010, IEEE, pp. 1-4.

GE, S.S. and CUI, Y.J., 2002. Dynamic motion planning for mobile robots using potential field method. *Autonomous robots,* **13**(3), pp. 207-222.

HERNÁNDEZ-MARTÍNEZ, E.G. and ARANDA-BRICAIRE, E., 2011. Convergence and collision avoidance in formation control: A survey of the artificial potential functions approach. *Multi-Agent Systems-Modeling, Control, Programming, Simulations and Applications.* InTech, .

HOU, Y. and ALLEN, R., 2008. Intelligent behaviour-based team UUVs cooperation and navigation in a water flow environment. *Ocean Engineering,* **35**(3-4), pp. 400-416.

KANJANAWANISHKUL, K., 2016. Formation control of mobile robots: Survey. *Journal of Engineering,* **4**(1), pp. 50-64.

KOREN, Y. and BORENSTEIN, J., 1991. Potential field methods and their inherent limitations for mobile robot navigation, *Robotics and Automation, 1991. Proceedings., 1991 IEEE International Conference on* 1991, IEEE, pp. 1398-1404.

LIU, Y. and BUCKNALL, R., 2016. The angle guidance path planning algorithms for unmanned surface vehicle formations by using the fast marching method. *Applied Ocean Research,* **59**, pp. 327-344.

LIU, Y. and BUCKNALL, R., 2015. Path planning algorithm for unmanned surface vehicle formations in a practical maritime environment. *Ocean Engineering,* **97**, pp. 126-144.

MOHAMMADI, A. and MENHAJ, M.B., 2013. Formation control and obstacle avoidance for nonholonomic robots using decentralized mpc, *Networking, Sensing and Control (ICNSC), 2013 10th IEEE International Conference on* 2013, IEEE, pp. 112-117.

MURRAY, R.M., 2007. Recent research in cooperative control of multivehicle systems. *Journal of Dynamic Systems, Measurement, and Control,* **129**(5), pp. 571-583.

PARK, B.S., 2015. Adaptive formation control of underactuated autonomous underwater vehicles. *Ocean Engineering,* **96**, pp. 1-7.

PARKER, L.E., 2000. Current state of the art in distributed autonomous mobile robotics. *Distributed Autonomous Robotic Systems 4.* Springer, pp. 3-12.

PRADHAN, S.K., PARHI, D.R., PANDA, A.K. and BEHERA, R.K., 2006. Potential field method to navigate several mobile robots. *Applied Intelligence,* **25**(3), pp. 321-333.

RADOVNIKOVICH, M. and CHEOK, K.C., 2014. Simultaneous multi-vehicle control and obstacle avoidance using supervised optimal planning, *Technologies for Practical Robot Applications (TePRA), 2014 IEEE International Conference on* 2014, IEEE, pp. 1-6.

REN, W., 2007. Multi-vehicle consensus with a time-varying reference state. *Systems & Control Letters,* **56**(7-8), pp. 474-483.

REN, W. and BEARD, R.W., 2008. *Distributed consensus in multi-vehicle cooperative control.* Springer.

REN, W., BEARD, R.W. and ATKINS, E.M., 2007. Information consensus in multivehicle cooperative control. *IEEE Control Systems,* **27**(2), pp. 71-82.

Appendix A

Graph theory notations (Ren, Beard 2008)

To describe information exchange among ships in terms under communication environment, graph theory is widely used. There are two types of graphs, directed and undirected graph. A directed graph is a graph that is a set of nodes connected by edges, where the edges have a direction associated with nodes. On the other hand, the edges of undirected graph can share information with each node linked by edges, because they have no direction between nodes.

A directed graph has nodes and edges that is a pair (N, E), where $\mathrm{N} = \{1, \dots, n\}$ is a set of nodes and $\mathrm{E} \subset \mathrm{N} \times \mathrm{N}$ is an edge set of ordered pairs of nodes, called edges. The edge $(i, j) \in \mathrm{E}$ indicates that node j called the child node can acquire state information from node i called the parent node and self-edges $(i, i) \in \mathrm{E}$ can be allowed. In terms of undirected graph, edges of an undirected graph do not have orientation and the pairs of nodes in the edges are not ordered. It means that node i and node j can get information from each other.

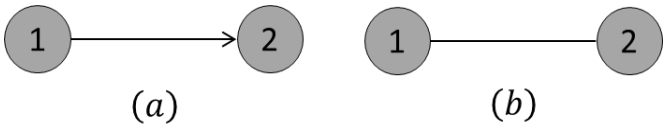

Figure A.1 Subplot (a) is a directed graph and subplot (b) is an undirected graph

Figure A.1 shows two different types of graph for two nodes represented by circle 1 and circle 2 and one edge depicted by an arrow and a line. Subplot (a) describes that the parent node1 gives information the child node2 and subplot (b) illustrates that node1 and node2 share information from each other.

To represent a graph in graph theory, an adjacency matrix $\mathrm{A} = [a_{ij}] \in R^{n \times n}$ of a directed graph with node set $\mathrm{N} = \{1, \dots, n\}$ is widely used. The adjacency matrix is a square matrix of components a_{ij} , where $a_{ij} = 1$ if $(j, i) \in E$, while $a_{ij} = 0$ if $(j, i) \notin E$ and in terms of self-edges, $a_{ii} > 0$. In Figure A.1 (a) and (b), adjacency matrix $\mathrm{A} = \begin{bmatrix} c & 0 \\ 1 & c \end{bmatrix}$ in directed graph and $\mathrm{A} = \begin{bmatrix} c & 1 \\ 1 & c \end{bmatrix}$ in undirected graph, where $\mathrm{c} > 0$, respectively.

In graph theory, a tree consists of a rooted node, the other nodes and edges between all nodes. If a tree may have orientation, it is called a directed tree. A rooted node is a node which has been picked as one parent node of the tree. The rooted node can access to every nodes in the tree and give state information to all nodes. A tree that is a subgraph G_s including all nodes with minimum edges of the graph G is called a spanning tree of the graph G. Therefore, a spanning tree does not contain cycles and disconnection.

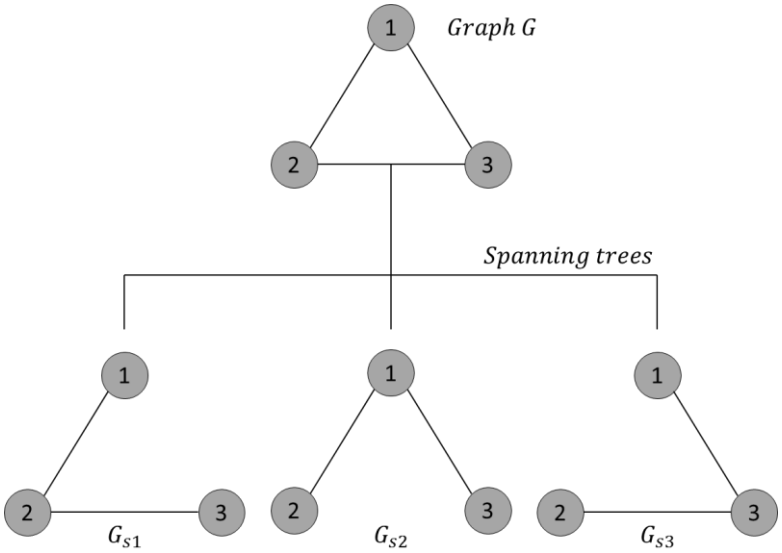

Figure A.2 A connected graph and possible spanning trees

In Figure A.2, fully connected graph G has three possible candidates of a spanning tree, G_{s1}, G_{s2} and G_{s3}. The spanning tree has following characteristics. The first characteristic is that the spanning tree will be disconnected when an edge of the spanning tree is removed. Another characteristic is that the spanning tree will be a circular loop when an edge of the spanning tree is added.

Appendix B

Fundamental consensus algorithm (Ren, Beard et al. 2007)

In order to achieve synchronization among ships, we need consensus algorithm to share state information with a fleet of ships. Suppose that we have n ships in a fleet. To describe communication environment among ships, we use a directed graph G that consists of (V, E), where $V = \{1, \ldots, n\}$ is the node set and $E = V \times V$ is the edge set. To model mathematically the communication environment, we let $A = [a_{ij}] \in \mathbb{R}^{n \times n}$ be an adjacency matrix. The communication environment may be varying in time because of vehicle motion or communication drop out. However, the communication environment will not change for simplified simulation in this study. Therefore adjacency matrix A is not time-varying matrix. The following equations are the most common consensus algorithm and single-integrator dynamics.

$$\dot{x}_i = u_i, \quad i = 1, \ldots, n \tag{B.1}$$

$$\dot{x}_i(t) = -\sum_{j=1}^{n} a_{ij}(x_i(t) - x_j(t)), \quad i, j = 1, \ldots, n \tag{B.2}$$

In equation (B.1), $x_i \in \mathbb{R}^m$ is the information state and $u_i \in \mathbb{R}^m$ is the control input of the i^{th} ship in a fleet. In equation (B.2), a_{ij} is the (i, j) entry of the adjacency matrix $A \in \mathbb{R}^{n \times n}$ and $x_{i,j}(t) \in \mathbb{R}^m$ is the information state of the i^{th}, j^{th} ships at time t. If $(j, i) \in E$, $a_{ij} = 1$ otherwise, $a_{ij} = 0$ that means the j^{th} ship cannot give the information state to the i^{th} ship, $\forall j \neq i$. Instinctively, the information state of each ship of equation (B.2) converges towards the neighbours' information state. The information state of a fleet of ships can meet at a common value if all $x_i(0)$ exist and $\| x_i(t) - x_j(t) \| \to 0$ as $t \to \infty$ where $i, j = 1, \ldots, n$. However, it does not guarantee the specified common value and convergence time.

We have a simple scenario to describe basic consensus algorithm for six point mass models based on two equations (B.1) and(B.2). Initial positions of the six models are $(0.1, 0)$, $(0.3, 0)$, $(0.5, 0)$, $(0.7, 0)$, $(0.9, 0)$ and $(1.1, 0)$, respectively. A graph G is shown in below figure.

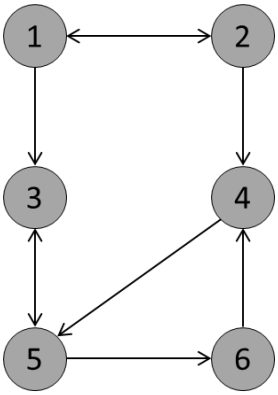

Figure B.1 Communication interaction among the six models

Figure B.1 shows time invariant communication topology among the models. The graph G has a directed spanning tree structure, therefore it can share their x direction position information with all neighbours.

$$A=\begin{bmatrix} -1 & 1 & 0 & 0 & 0 & 0 \\ 1 & -1 & 0 & 0 & 0 & 0 \\ 1 & 0 & -2 & 0 & 1 & 0 \\ 0 & 1 & 0 & -2 & 0 & 1 \\ 0 & 0 & 1 & 1 & -2 & 0 \\ 0 & 0 & 0 & 0 & 1 & -1 \end{bmatrix} \tag{B.3}$$

Equation (B.3) shows an adjacency matrix $A \in \mathbb{R}^{6\times 6}$ associated with the graph G .

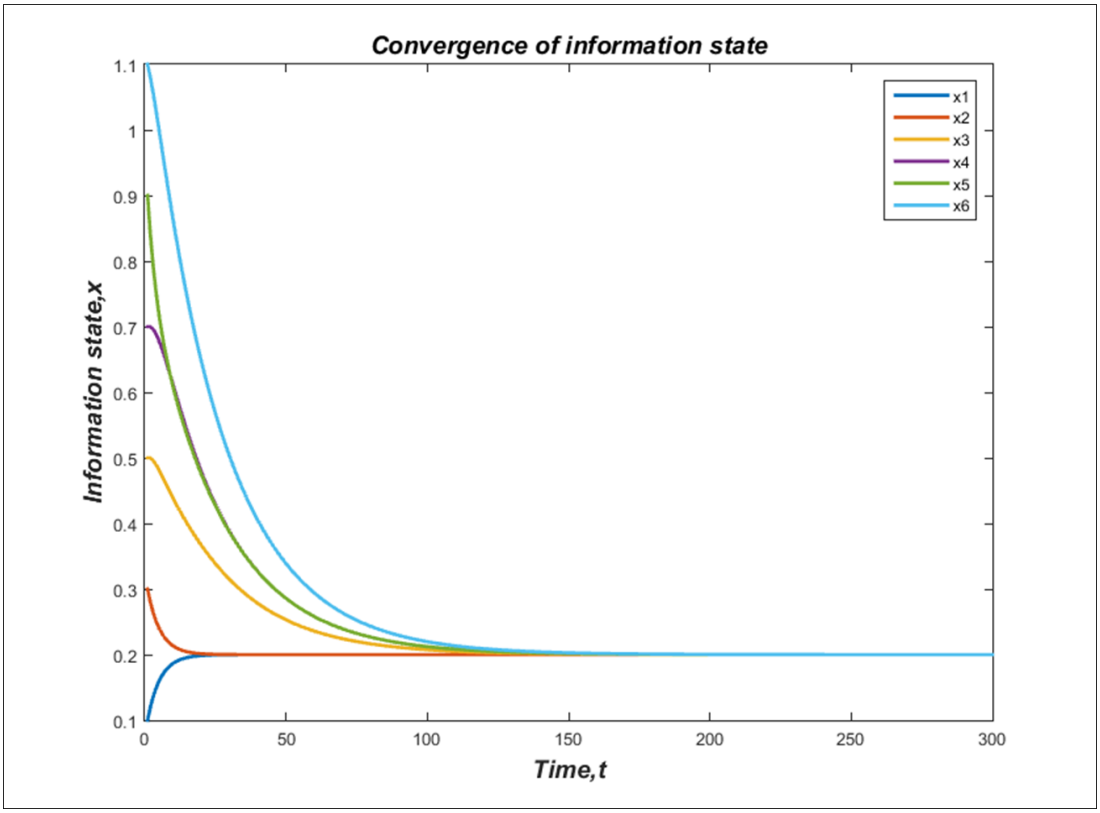

Figure B.2 Result of Information state for six point mass models

Figure B.2 shows the result of x position information for the models based on equation (B.1) and (B.2). The six models converge at a point 0.2 which is an average between initial positions of model 1 and model 2, because two models meet faster than other models and then other models move to the point.

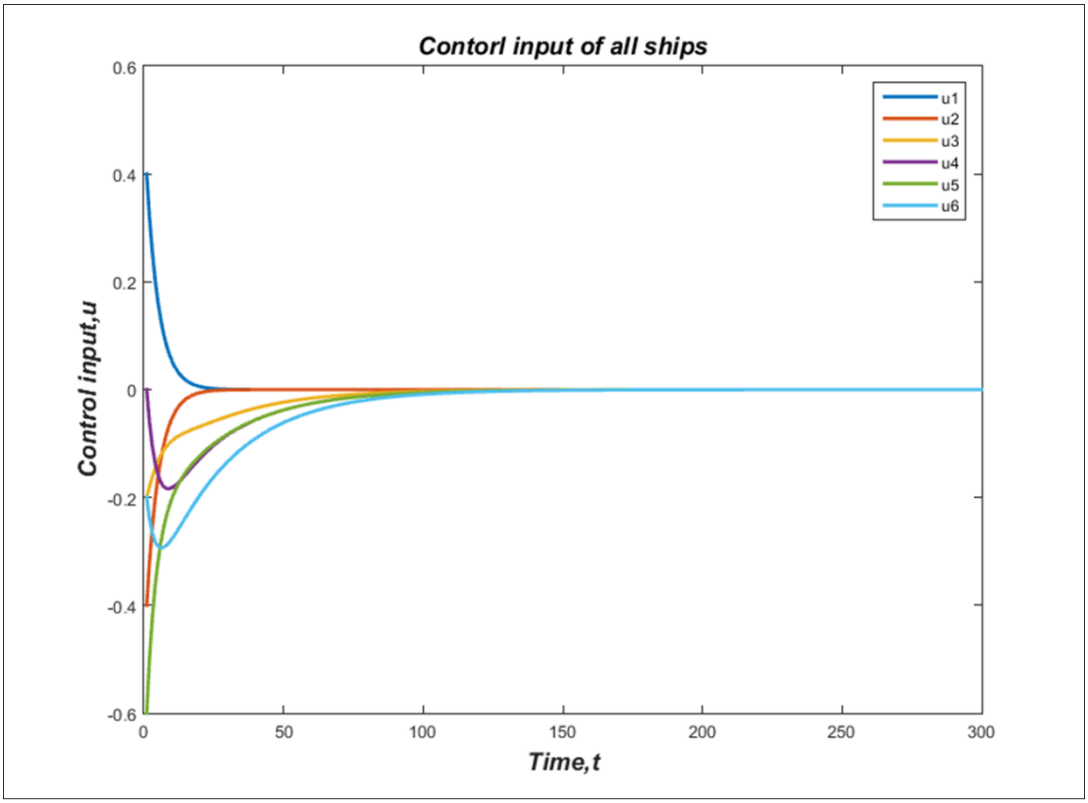

Figure B.3 Result of control input for six point mass models

Figure B.3 shows the result of control inputs converging at zero point. Model 1 only has positive control input and the others have negative control inputs to move in negative direction. The control inputs of the models achieve consensus perfectly after $t = 150s$. It means that the models do not move after consensus is reached completely.

Appendix C

Extended consensus algorithm (Ren 2007)

Equations (B.1) and (B.2) guarantee the convergence of the basic consensus algorithm, if the models have initial positions and a graph is a directed spanning tree structure. However, the common value of consensus for the models cannot be specified and variable. Therefore, formation control based on consensus algorithm need an improved equation that can specify a reference state as a common value.

The equation of single-integrator dynamics is given by

$$\dot{\xi}_i = u_i, \qquad i = 1,\ldots,n \tag{C.1}$$

Where $\xi_i \in \mathbb{R}^n$ is the information state representing x and y position and u_i is the control input of the i^{th} model. In addition, there is an additional model labelled n+1, which is designated as a leader that acts as a reference information state. Accordingly, the information state of the leader has the reference information state $\xi_{n+1} \triangleq \xi^r \in \mathbb{R}^m$, where ξ^r means the reference state of consensus.

The control objective of tracking a leader is $\zeta_i(t) \to \zeta^r(t)$, $i = 1,\ldots,n$, as $t \to \infty$. In terms of a directed spanning tree graph that is equivalent to the condition that the only one leader have a directed path to all the other followers, The graph is given by $G_{n+1} \triangleq (V_{n+1}, E_{n+1})$, where $V_{n+1} = \{1,\ldots,n+1\}$ is the node set and $E_{n+1} \subseteq V_{n+1} \times V_{n+1}$ is the edge set. An adjacency matrix associated with G_{n+1} is given by $A_{n+1} = [a_{ij}] \in \mathbb{R}^{(n+1)\times(n+1)}$, where $a_{ij} > 0$ if $(j,i) \in E_{n+1}$ and $a_{ij} = 0$ otherwise for all $i = 1,\ldots,n$ and $j = 1,\ldots,n+1$ in addition to $a_{(n+1)j} = 0$ for all $j = 1,\ldots,n+1$.

The control input equation is considered in this algorithm for tracking the reference state,

$$u_i = \frac{1}{\eta_i}\sum_{j=1}^{n} a_{ij}[\dot{\xi}_j - (\xi_i - \xi_j)] + \frac{1}{\eta_i} a_{i(n+1)}[\dot{\xi}^r - (\xi_i - \xi^r)], \quad i = 1,\ldots,n \tag{C.2}$$

Where a_{ij} is the (i,j) entry of the adjacency matrix A_{n+1}, $i = 1,\ldots,n$ and $j = 1,\ldots,n+1$, $\eta_i \triangleq \sum_{j=1}^{n+1} a_{ij}$. In addition, the derivative of the information state is given by $\dot{\xi}_j = \dfrac{\xi_j(k+1) - \xi_j(k)}{h}$, where k is the discrete-time index and h is the sampling time of

simulation. Simulation assumes that $a_{i(n+1)} = 1$ if $(n+1, i) \in E_{n+1}$ and $a_{i(n+1)} = 0$ otherwise. It is noticeable that each vehicle's control input is related with its neighbours' information states and their derivatives because of the tracking characteristic of (C.2).

A simple scenario shows trajectory of a time varying reference state for one leader and four followers under fixed communication environment. The leader is designated as model 5 and the followers are model 1, model 2, model 3 and model 4. Initial positions of the five models are $(1.5,0)$, $(0.5,0)$, $(0,0)$, $(-0.5,0)$ and $(1,0)$, respectively. Additionally, the time-varying reference state is shown by $\xi_5 = \xi^r(t) = \cos(t)$. A directed spanning tree graph is described in below figure.

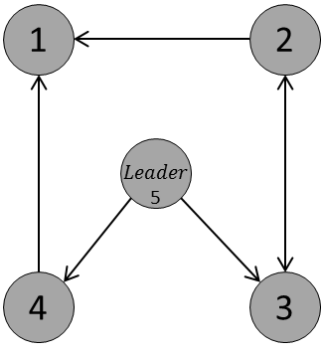

Figure C.1 Communication topology for the five models

The leader shares its information state with model 3 and model 4. Model 1 and model 2 can obtain the information states of model 4 and model 3, respectively. Therefore, the four followers can get the information state of the leader. Accordingly, the graph ensures that the followers can converge toward the reference state. The adjacency matrix associated with the graph is given by

$$A = \begin{bmatrix} 0 & 1 & 1 & 1 & 0 \\ 0 & 0 & 1 & 0 & 0 \\ 0 & 1 & 0 & 0 & 1 \\ 0 & 0 & 0 & 0 & 1 \\ 0 & 0 & 0 & 0 & 0 \end{bmatrix} \quad \text{(C.3)}$$

As a result in this scenario, the information states of the five models are depicted in below figure.

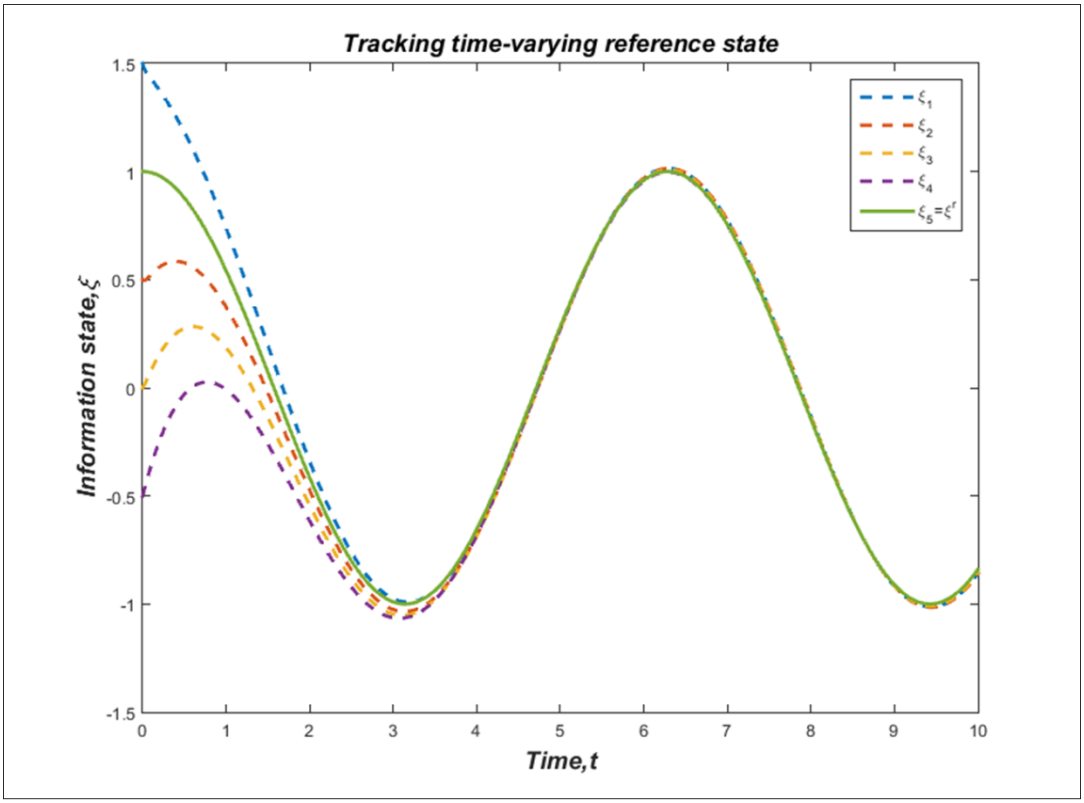

Figure C.2 Information states of followers to track reference state

Where the information states of the followers are represented by dotted lines and the reference state is drawn by a solid line. Figure C.2 shows that the followers located in different points at the first tend to rendezvous asymptotically.

Appendix D

Detail descriptions of the behaviours for the fleet in interval A-E

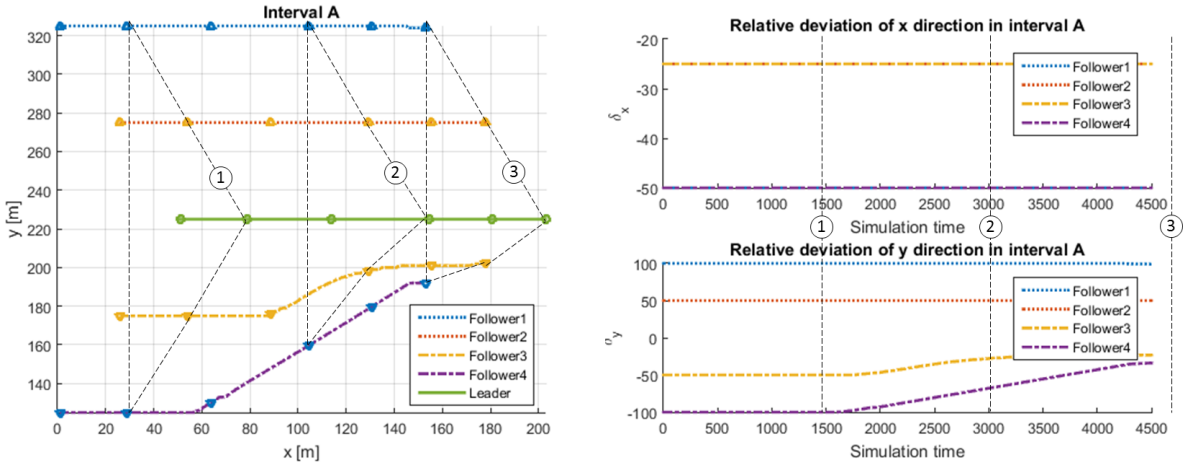

Figure D.1 Coordinated paths and relative deviations in interval A

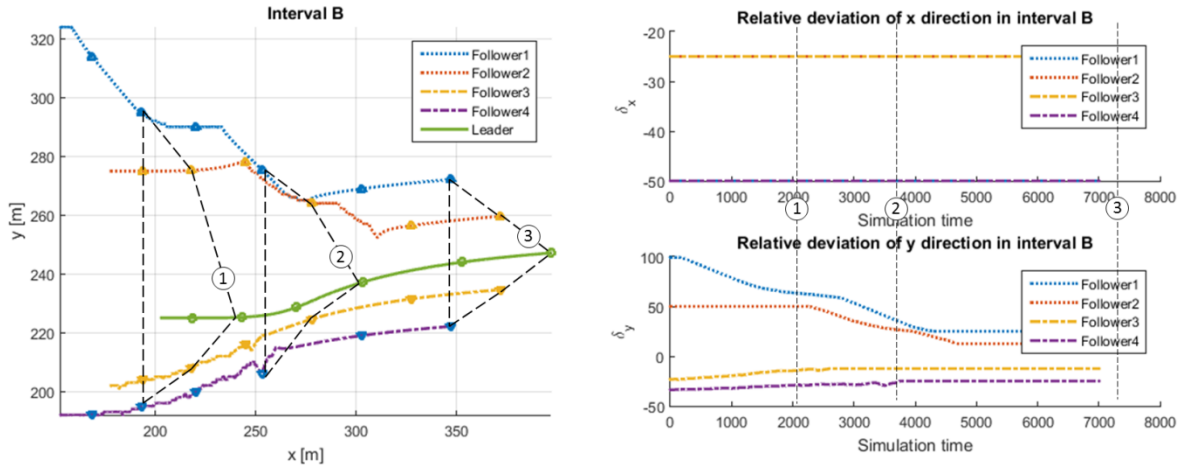

Figure D.2 Coordinated paths and relative deviations in interval B

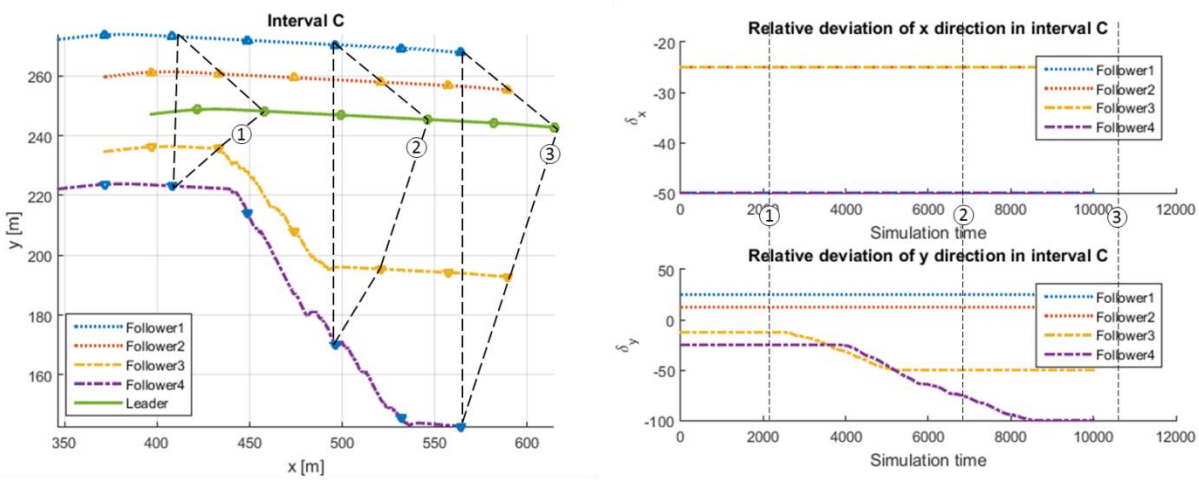

Figure D.3 Coordinated paths and relative deviations in interval C

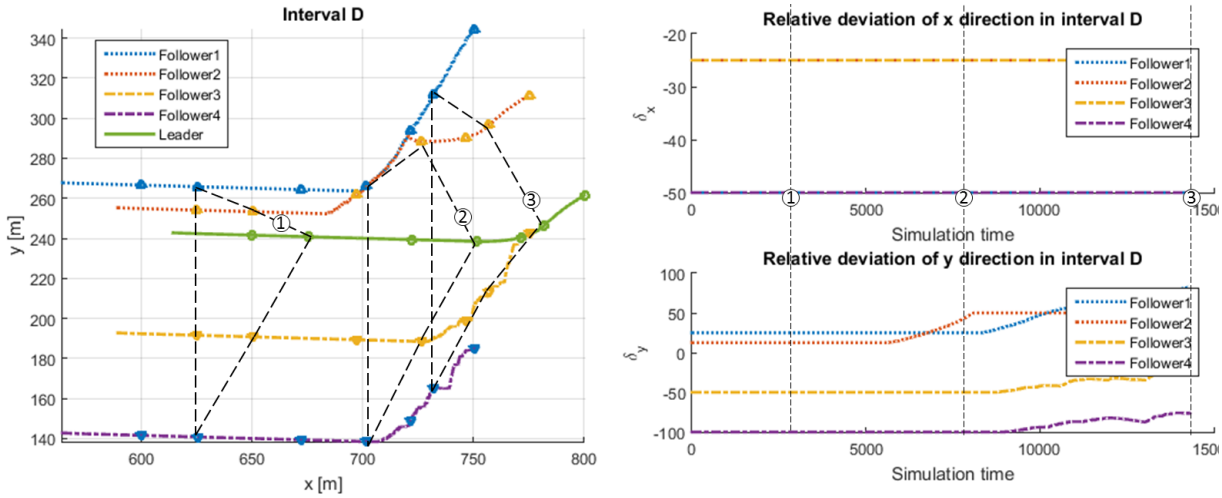

Figure D.4 Coordinated paths and relative deviations in interval D

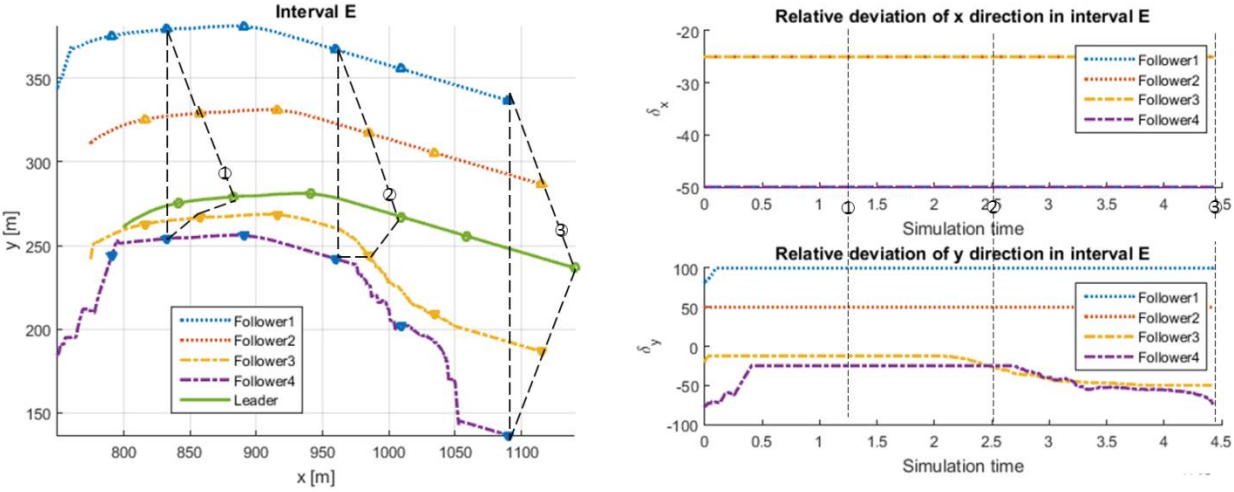

Figure D.5 Coordinated paths and relative deviations in interval E

Appendix E

Matlab Code for simulations

E-1. MATLAB Code for coordinated path planning strategy

```
%% Generate a path for leader using PFM
% % % % % % % % Initialization and basic setting % % % % % % % % % % % % %
close all
clear all
clc

map=imread('Simulation.bmp'); % map reading

start=[50,225]; % start point
goal=[1190,225]; % goal point

[Att,Rep,Tot,route,GDx,GDy,GDobx,GDoby]= PFM(map,start,goal);

figure(1);
imshow(map); % plotting map
figure(2);
mesh(Att);
figure(3);
mesh(Rep);
figure(4);
mesh(Tot);

figure(5);
quiver(GDx,GDy,0.5);
figure(6);
quiver(GDobx,GDoby,0.5);

figure(7);
hold on; quiver(GDx,GDy,0.5)
ps = plot(start(1), start(2), 'ro', 'MarkerSize', 9);
pg = plot(goal(1), goal(2), 'b*', 'MarkerSize', 9);
p3 = plot (route(:,1), route(:,2), 'k', 'LineWidth', 2); hold off;

%% Generate a path for a fleet of vehicles using consensus algorithm based
on PFM

n=5; % # of vehicles
A=[ 0 0 1 0 1
    0 0 1 0 1
    0 1 0 0 1
    1 0 0 0 1
    0 0 0 0 0];

k=1; dt=0.01;
k_end=length(route);

x(1:n,1)=[1;26;26;1;51];
y(1:n,1)=[325;275;175;125;225];
dx(n,1)=0; dy(n,1)=0; % dx,dy: reference x,y derivative
```

```
deltax_max1(1:n-1,1) = [-50;-25;-25;-50]; deltay_max1(1:n-1,1) = [100;50;-
50;-100;]; % Second formation shape
% deltax_min1(1:n-1,1) = [-50;-25;-12.5;-37.5]; deltay_min1(1:n-1,1) =
[0;0;0;0]; % First formation shape
deltax_min1(1:n-1,1) = [-50;-25;-25;-50]; deltay_min1(1:n-1,1) = [25;12.5;-
12.5;-25]; % First formation shape

deltax(1:n-1,1)=deltax_max1(1:n-1,1); deltay(1:n-1,1)=deltay_max1(1:n-1,1);
Ddeltax(1:n-1,1)=0; Ddeltay(1:n-1,1)=0;

ux=zeros(n,k_end); uy=zeros(n,k_end);
eta=[2;2;2;2;0];

while k ~= k_end

        for i=1:n-1;

            deltax_max=deltax_max1(i,1); deltay_max=deltay_max1(i,1);
            deltax_min=deltax_min1(i,1); deltay_min=deltay_min1(i,1);
            F1=[deltax_min1(i,1)-deltax_max1(i,1), deltay_min1(i,1)-
deltay_max1(i,1)];
            R=[GDobx(ceil(y(i,k)),ceil(x(i,k))),
GDoby(ceil(y(i,k)),ceil(x(i,k)))];


[deltax1,deltay1]=delta(deltax_max,deltay_max,deltax_min,deltay_min,R,F1);

            deltax(i,k+1)=deltax1; deltay(i,k+1)=deltay1;

            Ddeltax(i,k)=(deltax(i,k+1)-deltax(i,k))/dt;
            Ddeltay(i,k)=(deltay(i,k+1)-deltay(i,k))/dt;
            Ddeltax(i,k) = min(2.5,max(-2.5,Ddeltax(i,k)));
            Ddeltay(i,k) = min(2.5,max(-2.5,Ddeltay(i,k)));

            deltax(i,k+1)=deltax(i,k)+Ddeltax(i,k)*dt;
            deltay(i,k+1)=deltay(i,k)+Ddeltay(i,k)*dt;

               for j=1:n-1;
                   ux(i,k+1)=ux(i,k)+A(i,j)*(ux(j,k)-Ddeltax(j,k)-
1*((x(i,k)-x(j,k))-(deltax(i,k+1)-deltax(j,k+1))));
                   uy(i,k+1)=uy(i,k)+A(i,j)*(uy(j,k)-Ddeltay(j,k)-
1*((y(i,k)-y(j,k))-(deltay(i,k+1)-deltay(j,k+1))));
               end

            ux(i,k+1) =
Ddeltax(i,k)+1/eta(i,1)*ux(i,k+1)+1/eta(i,1)*A(i,n)*(dx(1,k)-1*(x(i,k)-
deltax(i,k+1)-x(n,k)));
            uy(i,k+1) =
Ddeltay(i,k)+1/eta(i,1)*uy(i,k+1)+1/eta(i,1)*A(i,n)*(dy(1,k)-1*(y(i,k)-
deltay(i,k+1)-y(n,k)));

            ux(i,k+1) = min(8,max(-8,ux(i,k+1)));
            uy(i,k+1) = min(8,max(-8,uy(i,k+1)));

            x(i,k+1)=x(i,k)+ux(i,k+1)*dt;
            y(i,k+1)=y(i,k)+uy(i,k+1)*dt;
        end
```

```
    x(n,k+1)=route(k+1,1);
    y(n,k+1)=route(k+1,2);
    dx(1,k+1)=(x(n,k+1)-x(n,k))/dt;
    dy(1,k+1)=(y(n,k+1)-y(n,k))/dt;

    k=k+1;

end
```

E-2. MATLAB Code for 'Potential field method'

```
function [ attractive,repulsive,f,route,gx,gy,gx_ob,gy_ob ] =
PFM( map,start,goal )
%UNTITLED4 Summary of this function goes here
%   Detailed explanation goes here
[xx,yy]=meshgrid(1:length(map(1,:)),1:length(map(:,1))); % generate grid
from bitmap to matlab environment.

    nu1=0.20*0.008; % attractive strength

attractive=nu1*((xx-goal(1)).^2+(yy-goal(2)).^2); % caculate attractve
force

obs=~map; % representation of obstacles in the matlab
obs=obs(end:-1:1,:); % to fit bitmap and matlab
d=bwdist(obs); % calculate distance between obstacle and point

    d2 = d/50 + 1; % arbitrary values
    d0 = 2; % influence of obstacle parameter
    nu = 350; % repulsive strength

repulsive = nu*((1./d2 - 1/d0).^2); % repulsive force
repulsive (d2 > d0) = 0;

f=attractive+repulsive;


[gx,gy]=gradient(-f);
[gx_ob,gy_ob]=gradient(-repulsive);

    i_max=100000;
    i=1; %current iteration

route=start;
current_pos=start; %current position

while i<i_max && norm(goal-current_pos)>3.0
    %current position
    j=round(current_pos(1));
    k=round(current_pos(2));

    Advance = [gx(k,j),gy(k,j)];
    current_pos =current_pos + 0.01*Advance;
```

```
    route=[route;current_pos];

    i=i+1;
end

end
```

E-3. MATLAB Code for ‘adjusted relative deviations’

```
function [deltax1,deltay1] =
delta(deltax_max,deltay_max,deltax_min,deltay_min,R,F1)
%UNTITLED3 Summary of this function goes here

if R==0;
    % Without repulsive force, formation shape is the second one
    deltax1=deltax_max; deltay1=deltay_max;
else
    % With repulsive force, formation shape goes the first one from the
second one

    % To calculate an angle(theta) btw vectors (F1 and R)
    s=cross([F1 0],[R 0]); ss=sign(s(1,3));
    theta=ss*acos(dot(F1,R)/(norm(R)*norm(F1)));

    % To calculate an angle(phi)
    s1=cross([1 0 0],[F1 0]); ss1=sign(s1(1,3));
    phi=ss1*acos(dot(F1,[1 0])/(norm(F1)*1));

    % To update deltax,deltay of shape formation
    deltax0 = 100*norm(R)*cos(theta)*cos(phi);
    deltay0 = 100*norm(R)*cos(theta)*sin(phi);

    deltax1 = min(deltax_min, max(deltax_max,deltax_max+deltax0));
    deltay1 = min(deltay_min, max(deltay_max,deltay_max+deltay0));

end
end
```